OPERATION OF OVER-CURRENT RELAYS DURING DOUBLE-PHASE OPERATION MODE OF POWER DISTRIBUTION SYSTEMS

SEYEDAHMAD HAJISEYEDOLIA

A THESIS SUBMITTED TO THE FACULTY OF GRADUATE STUDIES
IN PARTIAL FULFILMENT OF THE REQUIREMENTS
FOR THE DEGREE OF

MASTERS OF APPLIED SCIENCE

GRADUATE PROGRAM IN ELECTRICAL ENGINEERING AND COMPUTER SCIENCE
YORK UNIVERSITY
TORONTO, ONTARIO
AUGUST 2018

Abstract

Power system reliability is one of the objectives of every electric utility. The utilities attempt to maintain the continuity of power supply to their customers and minimize short-term or long-term power disruptions to the loads. Statistical analyses of actual faults in power systems demonstrate that most of the faults are asymmetrical, i.e., they include one or two phases only. Among asymmetrical faults, single-phase-to-ground short-circuits are the most common faults in distribution systems.

Conventional circuit breakers operate for all three phases. However, modern breakers are capable of disconnecting the faulted phase(s). Disconnection of faulted phase(s) increases the reliability of the system. However, a disconnected faulty phase can cause different challenges for distribution system like load imbalance and increase in the level of residual current. These challenges for distribution systems adversely affect the operation of protective devices.

In this research, the effects of operating the distribution system with a disconnected phase—known as double-phase operation mode (DPOM)—on operation of protective devices are ana-

lyzed. The protection devices investigated in this research are phase and earth fault over-current relays. Based on the effects of DPOM on operation of protective relays, a new method for setting the relays properly during DPOM is presented. This method provides the relays with proper settings during DPOM to guarantee the reliability of the protection system. To this aim, two type of settings, called "prompt settings" and "optimum settings" are presented to coordinate the relays during DPOM. Prompt settings are applied immediately after the detection of DPOM; optimum settings are applied when appropriate signals are received via the communication network. As a result, the communication bandwidth required by this method is minimal.

This method is evaluated for grounded distribution systems, which are the most common type of distribution systems in North America. For this purpose, the North-American version of the CIGRE medium-voltage (MV) benchmark system is modeled using PSCAD/EMTDC program. The results prove that the proposed method is capable of re-coordinating the protective relays during DPOM for both radial and meshed configurations of distribution systems with or without the presence of distributed generation units.

Acknowledgements

I would first like to thank my thesis advisor Dr. Ali Hooshyar of the Lassonde School of Engineering at York University. The door to Prof. Hooshyar's office was always open whenever I ran into a trouble spot or had a question about my research or writing. He steered me in the right direction during this two years of my graduate studies whenever he thought I needed it. I learned a lot from him, both in research and in having a professional life-style as a researcher.

I would also like to thank the thesis evaluation committee who were involved in the validation survey for this research project: Dr. John Lam. Without their passionate participation and input, the validation survey could not have been successfully conducted.

I would also like to acknowledge Dr. Baoxin Hu of the department of Earth and Space Science and Engineering at York as the second reader of this thesis, and I am gratefully indebted to her for her very valuable comments on this thesis.

Finally, I must express my very profound gratitude to my parents with unfailing support and continuous encouragement throughout my years of study. They have participated in this success

more than anybody with their sacrifices and supports. This accomplishment would not have been possible without them. Also, my sisters, Meshkat and Mahyas, made this easier for me by their positive vibes and energy. Thank you.

Seyedahmad Hajiseyedolia

Contents

List of Tables

List of Figures

Abbreviations

Com Commercial

CTI Coordination Time Interval

DG Distributed Generation

DPOM Double-Phase Operation Mode

EI Extremely Inverse

Ind Industrial

MCDC Main Computer Data Center

MI Moderately Inverse

MV Medium Voltage

NSGA Non-dominant Sorting Genetic Algorithm

OBON Operated Breaker Order Number

PF Power Factor

PTDS Prompt Time Dial Setting

Res Residential

RON Relay Order Number

SLG Single-Line-to-Ground

SPRSPL Single-Phase-Reclosing-Single-Phase-Lockout

SPRTPL Single-Phase-Reclosing-Three-Phase-Lockout

TDS Time Dial Setting

TM Time Margin

TPRTPL Three-Phase-Reclosing-Three-Phase-Lockout

VI Very Inverse

Chapter 1

Introduction

1.1 Context

Power system reliability is one of the objectives of every utility. The utilities attempt continuity of power supply to their customers and minimize short-term or long-term power disruption to the loads connected to the system. To increase the reliability, the first step is studying the conditions that cause power disruption. A very common reason for outages is short-circuit faults. Statistical analyses of actual faults in power systems demonstrate that most of the faults are asymmetrical, i.e., they include one or two phases only [1]. Among asymmetrical faults, single-phase-to-ground short-circuits are the most common faults in distribution systems.

Protection systems are responsible for isolating faulty components, so the remainder of the

power grid can maintain its normal operation. Conventional protection systems of the grid disconnect all three phases during asymmetrical faults. In modern power systems, however, utilities are increasingly using single-pole breakers that are capable of disconnecting the faulted phase(s) only. Since a prime indicator of the reliability of a grid is the total outage time over certain time periods, disconnecting only the faulty phases during asymmetrical short-circuits improves the grid reliability considerably. An example of such improvement has been demonstrated for a four-wire multi-grounded medium-voltage distribution system in [1]. Operation of the single-pole breakers depends on the reclosing and lockout strategy that is applied to the network. Based on [1], there are three main reclosing-lockout strategies applied to the network.

- **Three-Phase-Reclosing-Three-Phase-Lockout (TPRTPL):**

  TPRTPL trips all the three phases of the system in case of a fault detection and if the fault is considered as permanent, all the three phases of the system will be locked out. This strategy is the conventional strategy of clearing the faulty part of the network. Although this strategy clears the fault from the rest of the network, it disconnects the healthy phases of the network as well during an asymmetrical fault. This strategy sacrifices the system reliability due to unnecessary disconnection of healthy phases of the system.

- **Single-Phase-Reclosing-Three-Phase-Lockout (SPRTPL):**

  Getting more popular among other reclosing-lockout strategies, SPRTPL trips and recloses only the faulted phase(s). In case of a permanent fault, however, all three phases of the system will be locked out. This strategy is similar to the scheme used for tripping-reclosing

of transmission lines.

- **Single-Phase-Reclosing-Single-Phase-Lockout (SPRSPL):**

  In this strategy, during a fault situation only the affected phase(s) by the fault will go through the tripping process and in case of a permanent fault, the faulted phase(s) will be locked out. This strategy improves the reliability of the system significantly since only the faulty phase(s) of the system are disconnected. On the other hand, this strategy can causes challenges to the network. For instance, suppose three-phase loads like three-phase motors are connected to the network. In case of an asymmetrical fault, disconnecting the damaged phase connects an unbalanced voltage to this motors that can cause severe damages. Other challenges like an increase in the level of zero-sequence current flowing through the network, malfunction of the protective devices and unbalanced situation for Distributed Generation (DG) units in the network are the consequences of this strategy of tripping-reclosing-lockout.

Reference [2] demonstrates the benefits of implementing reclosers with single-phase tripping single-phase lockout strategy on rural, residential and commercial distribution systems. In a rural distribution system for instance,c[2] proves that SPRSPL is beneficial on improvement of reliability. This improvement is obtained since in rural distribution systems typically large areas are covered by the lines, the following items increase the power outage time.

- **Fault locating and crews travel time:**

  In a rural network, usually the distribution feeders are longer and distances are higher. This

causes a significant increase in the needed time for locating the fault position. Furthermore, the travel time of maintenance crew is higher due to long distances.

- **Maintenance time:**

  The whole maintenance time in a rural network is more than an urban network since the distances are higher and take more time to fix the system.

By using breakers with SPRSPL, at least two-thirds of the load connected to the grid will not experience power outages.

Authors in [3] believe that expectations of the customers from the reliability of the service is high enough to consider SPRSPL or SPRTPL based on the loads connected to the network to minimize the temporary and permanent power outages. To reach this goal in [3], not only did they apply single-pole tripping-reclosing-lockout breakers, but also the breakers were placed in the optimum location. The optimum locations were obtained by benefiting from predictive reliability analysis on the test system. By finding the optimum location for the breakers and performing a reliability analysis on the test system, SPRTPL has improved the reliability of the system by 70%. SPRSPL strategy is also applied and the results of the reliability analysis show 80% improvement in reliability.

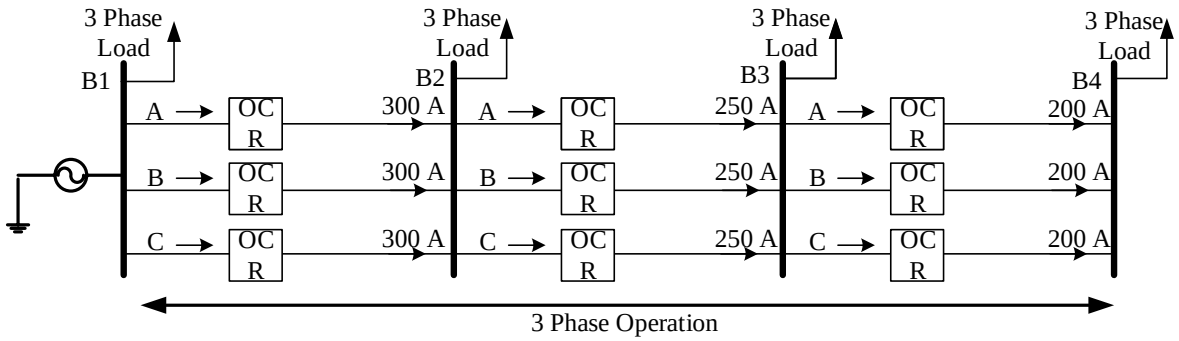

Figure 1.1: Diagram of the sample power network operating in three phase mode.

1.2 Challenges of DPOM for distribution systems

Although the advantages of single-pole tripping and reclosing schemes are widely recognized, there are drawbacks in operating the system with a disconnected phase. Operating the system with two-phase is called Double-Phase Operation Mode (DPOM). During DPOM, a part of the system operates with three-phase connected to the network and the rest operates with two healthy phases connected to the grid. Valid concerns are mentioned in the literature about applying single-pole tripping-reclosing and/or single-pole lockout on the power system. In [4] and [5] for instance, the following concerns are listed.

- **Load unbalance:**

  Power distribution engineers try to balance the loads that are connected to each phase of the system. For instance, suppose the single line diagram of the sample balanced network is given in figure 1.1. The amount of load current flowing through each phase is depicted in the diagram.

Now suppose a permanent Single Line to Ground (SLG) fault has happened on phase A of Bus B4. By applying SPRSPL strategy, phase A of the system has been disconnected from Bus B3. Figure 1.2 depicts the same network and shows the load current data on each phase.

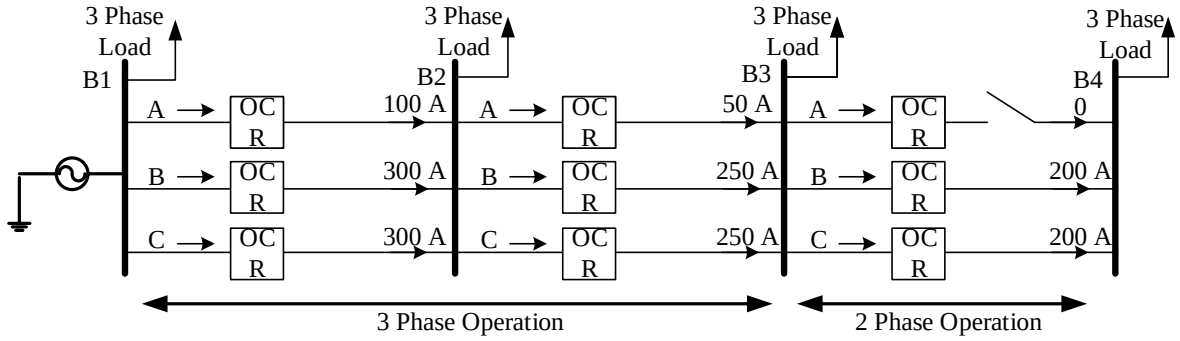

Figure 1.2: Diagram of the sample power network operating in double phase mode.

As it is illustrated in figure 1.2, since phase A between Bus B3 and B4 is disconnected from the rest of the network, the current flowing through phase A is less than the other phases of the system. As a result, the system is severely unbalanced. Operation of the system in such circumstances can cause the increment in the level of residual current flowing through the network which will be clarified in the next item.

- **Increase in the level of residual current:**

  Following the increment in the level of unbalanced load connected to the network, residual current flowing through the system increases. Residual current or zero-sequence current is the summation of the phasors of current of each phase. Equation (1.1) shows the

mathematical definition of zero-sequence current[6].

$$3I^0 = I_A + I_B + I_C \tag{1.1}$$

In this equation, I_A, I_B and I_C are phase A, B and C current phasors respectively. For example, for the balanced network depicted in figure 1.1, the residual current flowing through Bus B4 from Bus B3 is given in.1.2.

$$3I_o = I_A + I_B + I_C = 200\angle 0^\circ + 200\angle -120^\circ + 200\angle +120^\circ = 0 \tag{1.2}$$

Equation(1.2) shows that for this well-balanced sample network, when all the phases are connected, the zero-sequence current flowing through the network is zero. The zero-sequence current flowing through Bus B3 of the network after operation of the breaker in figure 1.2 is calculated in equation (1.3).

$$3I_o = I_A + I_B + I_C = 0 + 200\angle -120^\circ + 200\angle +120^\circ = 200\angle 180^\circ \tag{1.3}$$

As it is calculated in equation (1.3), a significant increase in the zero-sequence current flowing to the network will be sensed upon disconnection of a phase of the system. The severity of this shift depends on the current values of each phase before operation of the breaker as well.

The aforementioned side effects of using single-pole lockout strategies cause new challenges for the protective devices connected to the network. For such conditions, the reduction in the outage time as a result of SPRSPL adversely affects the performance of the protection system and so the intended improvement in reliability is not achieved. This is one of the main reasons for the

hesitation among some utilities about applying SPRSPL schemes. More details and explanations will be provided in next chapters for proving the poor performance of the protection system during DPOM.

1.3 Objectives

In this research, the effects of single-pole tripping-lockout schemes on the operation of protective devices in distribution systems are analyzed. In addition, a new methodology for setting the relays properly during DPOM is presented. Based on the literature, DPOM significantly increases the reliability of the system. However, as it was mentioned earlier, the operation of power system during DPOM causes malfunction of the protective relays. The objective of this project is to obtain a systematic methodology for finding a proper setting of protective relays during DPOM of distribution systems. This methodology should be able to promptly obtains new settings for the relays based on the new network parameters. Two critical factors must be considered in this methodology:

- **Benefiting from local measurement**

  Local measurement is referred to the parameters that a relay measures. These parameters include load current, sequence currents, busbar voltage and so on. The main parameter that is used for coordination of phase or sequence over-current relays is the load current and sequence currents, respectively. By benefiting from locally measured network

parameters, the necessary information for setting the relays during DPOM is provided.

- **Fast and reliable**

  It is vital to have the relays coordinated as soon as DPOM starts. Otherwise, the system will be left unprotected. Hence, the provided solution for re-coordination of the relays should be fast to guarantee the protection of the system.

To achieve the new settings based on the aforementioned factors, two sets of settings is proposed to be applied to the relays during DPOM.

- **Prompt settings**

  To ensure the protective relays are capable of protecting the system from the very first moment that DPOM starts, a prompt setting should be obtained by the relay based on the local measurements and DPOM start location. Prompt settings are the temporary settings that are available on the relays until the optimum settings are obtained and updated on all the relays of the network.

- **Optimum Settings**

  By applying the prompt settings on the relays of the network, the security of the system is ensured, however, the prompt settings are not necessarily the optimum settings that could be applied on the relays. Optimum settings in this project refer to the settings that minimize the operation time of the relays in the system. These settings and the method of obtaining them will be clarified in details shortly.

In this thesis, the term "protective devices" indicates the most commonly used relays in distribution systems, i.e., phase and earth-fault over-current relays. The rest of this chapter is organized as follow:

- Section 1.4 demonstrates the protection coordination during DPOM.
- Section 1.5 represents the outline of this thesis.

1.4 Methodology

The proposed methodology is as follows:

- **Mathematical formulation of short-circuit analysis for DPOM**

  Mathematical expressions of the network during DPOM for fault analysis is presented in this section.

- **Investigating the changes in network parameters caused by DPOM**

  Positive and zero-sequence currents are the main parameters used by utility engineers to set protective devices and coordinate them for protecting the system. To this aim, first of all, these changes should be investigated during DPOM.

- **Exploring the challenges for protective devices during DPOM**

  Due to the changes in system parameters, protective devices are subject to malfunction or

non-optimal operation. Thus, the challenges for protective devices during DPOM should be explored to re-coordinate these devices.

- **Presenting the new re-coordination methodology for protective devices**

  After studying the challenges for protective devices during DPOM, a new solution is presented for re-coordination of the protective devices. It is particularly essential for the proposed solution to use mainly locally measured quantities to decrease the implementation costs. This would also increase the speed of implementing the proper coordination scheme.

1.5 Thesis outline

The rest of this thesis is structured as follow:

- **Chapter 2: Mathematical modeling of DPOM**

  This chapter represents the mathematical formulation of the power system during DPOM using phase coordinate method [7][8][9], which will be the theoretical basis of this project.

- **Chapter 3: Addressing the challenges of DPOM for protective relays**

  In this chapter the challenges caused by DPOM on the operation of phase and earth overcurrent relays will be discussed. Case studies will be presented to show that the settings and methodologies for coordinating the relays over Three-phase Operation Mode (TPOM) are not applicable during DPOM.

- **Chapter 4: Re-coordination of over-current relays during DPOM**

  In chapter 3, the changes caused by DPOM on the distribution network were presented. The mentioned changes causes challenges on the operation of protective devices which were also discussed in chapter 3. Based on these studies, re-coordination of the over-current relays during DPOM is a critical action should be taken as soon as DPOM starts. In this chapter, a new methodology for re-coordination of the over-current relays is presented. Afterward, the methodology is evaluated by applying it on protective relays of the project test system.

- **Conclusion and future work**

  In this chapter, the concluded results from this research will be presented. Future research topics that can be conducted on this subject are also suggested at the end of this chapter.

Chapter 2

Mathematical modeling of DPOM

This chapter represents the mathematical formulation of the power system during DPOM using phase coordinate method [7][8][9], which will be the theoretical basis of this study. Section 2.1 discusses the fundamentals of phase coordinate method. In section 2.2, modeling process of distribution feeder is explained. Modeling of the distribution feeder is critical in this research since the operation of a breaker disconnects a phase of distribution feeder. This location of disconnection is the starting point of the zone operating in DPOM. In the next step, the modification process of the distribution feeder nodal admittance matrix during DPOM is performed. Nodal admittance matrix models the admittance of the distribution feeder between each node (phase). This process is shown in 2.3. To analyze the network fault behavior during DPOM, fault analysis process when the system is modeled by poly-phase nodal admittance matrix is presented in section 2.4. These studies are supported in section 2.5 by PSCAD/EMTDC simulation analysis of

sample power distribution network. The concluding remarks are elaborated in section 2.6.

2.1 Phase coordinate method

DPOM causes physical changes in the system since one of the conductors of the system is out of operation. To model these changes, a solution should be presented that benefits from the characteristics of each phase to model the system. Despite the conventional methods that transfer the system identities to symmetrical components, especially for short-circuit fault analysis studies, phase coordinate method models the power system components in the phase frame of reference. This modeling process starts with representing the poly-phase network conditions by the physical system identities, such as phase voltage, phase current and phase admittance/impedance. The following steps should be taken in order to model the system using the phase coordinate method.

- **Representing the system in phase-frame of reference**

  The first step is choosing the phase-frame of reference for the system. Modeling process of the system begins by choosing this reference. The term " phase-frame of reference" means the reference frame in which the system is modeled. Figure 2.1 depicts the three different phase-frame of references in a three-phase system. It is worth to mention that once the phase-frame of reference is chosen, it cannot be changed during the modeling process.

- **Obtaining the system nodal admittance matrix**

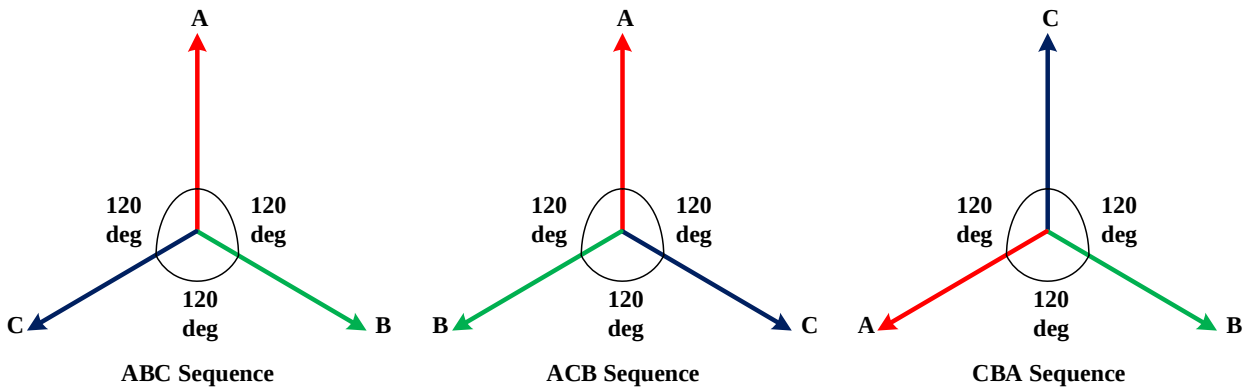

Figure 2.1: Different possible phase-frame of references.

In the second step, the nodal admittance matrix of the entire system is obtained. To do so, the admittance matrix of each equipment should be obtained. The admittance matrix of the whole system is obtained by integration of each equipment admittance matrix based on the connection points of the respective device.

- **Modifying the system nodal admittance matrix to model the changes cause by DPOM**

  During DPOM, modifications should be applied to the poly-phase nodal admittance matrix of the distribution system to model the disconnection of a line from the network.

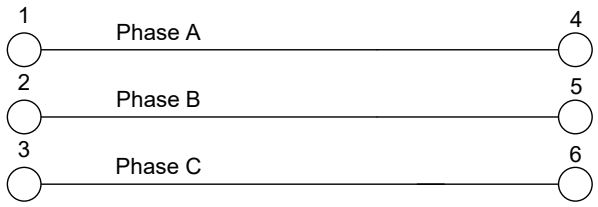

Figure 2.2: Three-phase distribution feeder nodal diagram.

2.2 Model of poly-phase admittance matrix of distribution feeder for TPOM

The most common model for distribution feeders is π-model [10]. A π-model circuit of a distribution feeder consists of series and parallel lumped admittance, which is used for modeling the feeder characteristics in the poly-phase nodal admittance matrix. The poly-phase admittance matrix of the distribution feeder is given by equation 2.1 for a three-phase distribution feeder with 6 nodes as depicted in figure 2.2.

$$Y_{TL} = \begin{vmatrix} Y_{abc} + \frac{1}{2} Y_{Cap} & -Y_{abc} \\ -Y_{abc} & Y_{abc} + \frac{1}{2} Y_{Cap} \end{vmatrix} \tag{2.1}$$

where,

$$Y_{abc} = \frac{1}{3} T.Y_{seq}.T^{*} \tag{2.2}$$

$$T = \begin{vmatrix} 1 & 1 & 1 \\ 1 & \alpha^2 & \alpha \\ 1 & \alpha & \alpha^2 \end{vmatrix} \tag{2.3}$$

where,

$$\alpha = 1\angle 120^o \tag{2.4}$$

$$Y_{seq} = \begin{vmatrix} y_0 & 0 & 0 \\ 0 & y_1 & 0 \\ 0 & 0 & y_2 \end{vmatrix} \tag{2.5}$$

As shown by equation (2.1), the distribution feeder poly-phase admittance matrix consists of four 3×3 sub-matrices which results in a 6×6 matrix. This matrix represents the total admittance between each node of the distribution feeder. In equation (2.1), Y_{Cap} represents the susceptance matrix of distribution feeder. Figure 2.3 depicts a schematic capacitive susceptances in $\frac{1}{2}.Y_{Cap}$ for a three-phase distribution feeder between two successive busbars. In distribution feeders, due to the short length of the lines, comparing with transmission lines, the $\frac{1}{2}.Y_{Cap}$ is negligible. Equation (2.2) represents the admittance matrix of the distribution feeder. In equation (2.2), T is the transformation matrix of sequence components and T^* is the conjugate transpose of matrix T. Equation (2.5) shows the diagonal sequence admittance matrix Y_{seq} which is used to find Y_{abc}.

To model the disconnected line of the network due to DPOM, modifications should be applied to the distribution feeder poly-phase admittance matrix. Section 2.3 describes this process.

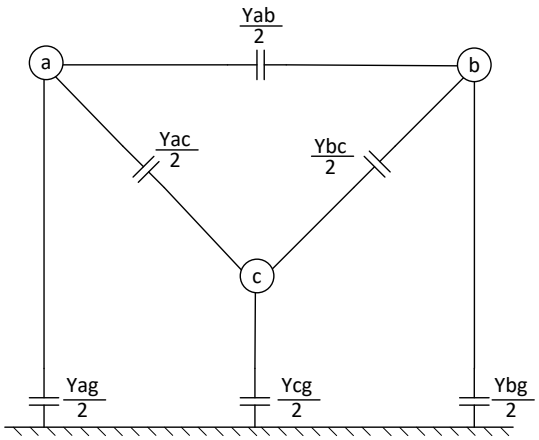

Figure 2.3: Equivalent capacitive susceptances between two successive Busbar.

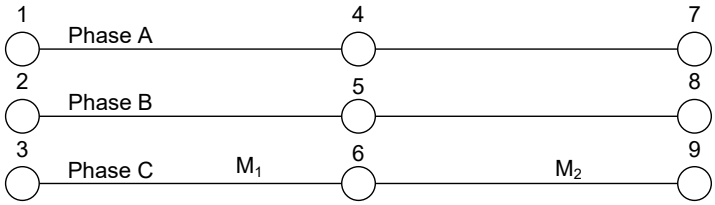

Figure 2.4: Nodal diagram of a distribution feeder during TPOM.

2.3 Modification to admittance matrix for DPOM

The effects of DPOM necessitates certain modifications on distribution feeder nodal admittance matrix. During TPOM, figure 2.4 shows the nodal diagram of a three-phase distribution feeder.

Now suppose that one phase of the distribution feeder is opened due to the operation of a single-pole breaker. Figure 2.5 illustrates the nodal diagram of a three-phase distribution feeder operating in DPOM. The opened phase adds a new node to the nodal model of the distribution feeder labeled as node 10 in figure 2.5. Presence of this new node changes the distribution feeder

nodal admittance matrix size by adding a new row and a column. Hence, the 9×9 admittance matrix turns into a 10×10 matrix. To find the elements of this new column, the conventional methodology presented in [11] is used. Equations (2.6)-(2.8) are presented here for clarifying the modification process of the distribution feeder admittance matrix.

Equation (2.6) shows that the admittance between node 10 and other nodes of the distribution feeder is equal to the admittance between node 6 and other nodes of the distribution feeder. Since there is no current flowing through node 6, the admittance is zero as it is shown in equation (2.6).

$$Y_{10,i} = Y_{6,i}; Y_{6,i} = 0; i = 7,8,9 \tag{2.6}$$

Equation (2.7) shows that the admittance matrix element $Y_{6,6}$ is the summation of the admittance between node 6 and nodes 1 to 5.

$$Y_{6,6} = \sum Y_{6,i}; i = 1,2,3,4,5 \tag{2.7}$$

Equation (2.8) shows that admittance matrix element $Y_{10,10}$ is the summation of the admittance between node 10 and nodes 4 to 9.

$$Y_{10,10} = \sum Y_{10,i}; i = 4,5,6,7,8,9 \tag{2.8}$$

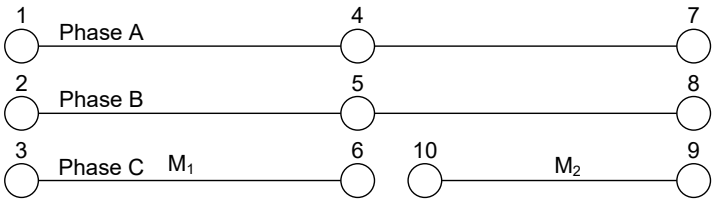

Figure 2.5: Changes on nodal diagram of a distribution feeder due to operation of a single-pole breaker.

2.4 Application of phase coordinate method for DPOM

To investigate the changes caused by DPOM in the behavior of the network during fault period, fault current calculation studies should be performed. To do so, after modifying the poly-phase admittance matrix of the distribution feeder, the voltages of each bus are obtained using equation (2.9).

$$YV = I \tag{2.9}$$

In equation (2.9), Y is the modified poly-phase nodal admittance matrix of the distribution feeder during DPOM. I and V are the column vectors of current and voltage respectively. Equation (2.9) is solved to find V, using pre-fault nodal current injections and poly-phase admittance matrix. Equation (2.10) is used for finding the current matrix I for each phase and node.

$$I_k = \frac{P_k - jQ_k}{V_k^*} \tag{2.10}$$

In equation (2.10) k is the node number and P and Q are the active and reactive power of each phase, respectively. After obtaining the pre-fault voltages during DPOM, suppose a single-phase-to-ground fault happens in the network. The fault current can be found by

Table 2.1: Network data.

Model	Z_0 (Ω)	Z_1 (Ω)	Z_2 (Ω)
Voltage source	0.064$\angle$80.5	0.08$\angle$80.5	0.08$\angle$80.5
Distribution feeder	0.4$\angle$71.6	0.162$\angle$69.1	0.162$\angle$69.1

$$I_{f_k} = \sum_{m=1}^{N} Y_{km} V_m \tag{2.11}$$

where f denotes fault condition and N is the total number of the nodes of the network.

2.5 Validation of the mathematical model

To show the accuracy of the above mathematical formulation, a sample network is modeled and simulated in PSCAD/EMTDC and the results of the fault current calculated by the phase coordinate method are compared with simulation results. Figure 2.6 depicts the configuration of the sample network, which includes a 220 kV voltage source along with an impedance, representing a Thevenin equivalent network, connected to a 1 km distribution feeder and a grounded Wye-delta 220kV/115 kV transformer. Table 2.1 presents the specifications of this network.

The base nodal admittance matrix of the network in figure 2.6 is obtained by combining the poly-phase nodal admittance matrices of the generator, distribution feeder, and transformer. Equations (2.12)-(2.15) show the poly-phase nodal admittance matrices of these elements.

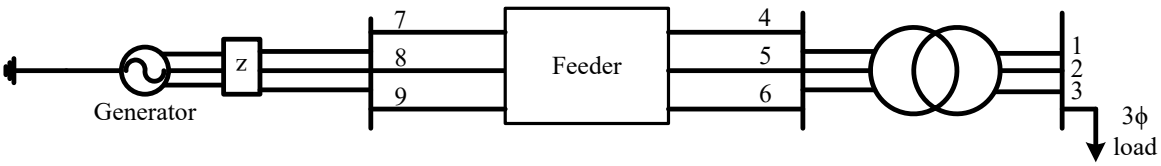

Figure 2.6: Sample network for evaluation of phase coordinate method.

$$Y_{Gen} = \begin{array}{c|ccc} NodeNumber & 7 & 8 & 9 \\ \hline 7 & 2.225-j13.34 & 0.1705-j1.026 & 0.1705-j1.026 \\ 8 & 0.1705-j1.026 & 2.225-j13.34 & 0.1705-j1.026 \\ 9 & 0.1705-j1.026 & 0.1705-j1.026 & 2.225-j13.34 \end{array} \tag{2.12}$$

$$Y_{Trans} = \begin{array}{c|cccccc} NodeNumber & 1 & 2 & 3 & 4 & 5 & 6 \\ \hline 1 & -j1.87 & j0.935 & j0.935 & 0 & j1.622 & -j1.622 \\ 2 & j0.935 & -j1.87 & j0.935 & -j1.622 & 0 & j1.622 \\ 3 & j0.935 & j0.935 & -j1.873 & j1.622 & -j1.622 & 0 \\ \hline 4 & 0 & -j1.622 & j1.622 & j2.809 & 0 & 0 \\ 5 & j1.622 & 0 & -j1.622 & 0 & -j2.809 & 0 \\ 6 & -j1.622 & j1.622 & 0 & 0 & 0 & -j2.809 \end{array} \tag{2.13}$$

By dividing the Y_{Trans} to four 3×3 sub-matrices, the following equivalent matrix is obtained:

$$Y_{Trans} = \begin{vmatrix} Y_{\mathrm{UL}} & Y_{\mathrm{UR}} \\ Y_{\mathrm{DL}} & Y_{\mathrm{DR}} \end{vmatrix} \tag{2.14}$$

where Y_{UL}, Y_{UR}, Y_{DL} and Y_{DR} are the up-left, up-right, down-left and down-right 3×3 sub-matrices, respectively.

Distribution feeder poly-phase nodal admittance matrix is obtained using equations (2.1) to (2.8). It is worth mentioning that the susceptance matrix of Y_{Cap} is neglected for the sake of simplicity in the calculations due to the short length of distribution feeders. Y_{abc} is given by equation (2.15) and feeder poly-phase nodal matrix is obtained by using Y_{abc} and equation (2.1).

$$Y_{abc} = \begin{vmatrix} 1.723 - j4.63 & -0.4675 + j1.1315 & -0.4675 + j1.1315 \\ -0.4675 + j1.1315 & 1.723 - j4.63 & -0.4675 + j1.1315 \\ -0.4675 + j1.1315 & -0.4675 + j1.1315 & 1.723 - j4.63 \end{vmatrix} \tag{2.15}$$

By obtaining the poly-phase nodal admittance matrices of the generator, the feeder, and the transformer, the base nodal admittance matrix of the network is given by:

$$Y_{Poly} = \begin{vmatrix} Y_{\mathrm{UL}} & Y_{\mathrm{UR}} & 0 \\ Y_{\mathrm{DL}} & Y_{\mathrm{DR}} + Y_{\mathrm{abc}} & -Y_{\mathrm{abc}} \\ 0 & -Y_{\mathrm{abc}} & Y_{\mathrm{abc}} + Y_{\mathrm{Gen}} \end{vmatrix} \tag{2.16}$$

By applying a single-phase-to-ground fault to the network during DPOM and through solving

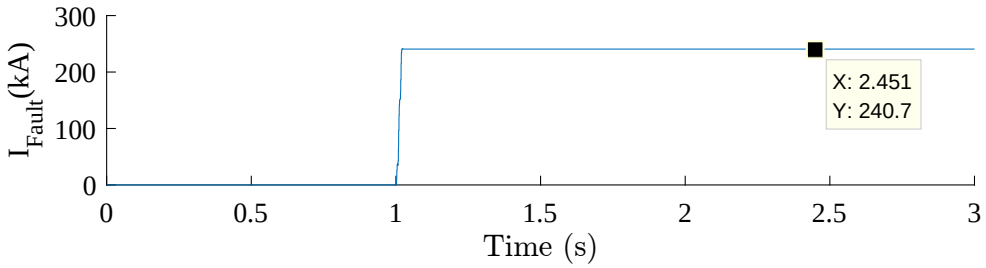

Figure 2.7: Fault current versus time for the sample system test.

equation (2.11), the calculated fault current is 241 A. Simulation results for this case shows a fault current of 240.7 A which is depicted in figure 2.7.

Comparing the simulation results and calculation results of single-phase-to-ground fault current during DPOM, the high accuracy of the phase coordinate method is concluded.

2.6 Conclusion

In this chapter, the mathematical basis for the calculations of the network during DPOM was presented. In the event of a DPOM, the poly-phase nodal admittance matrix of the system should be modified based on the equations represented in this chapter. A network analysis should be carried out based on the given methodology to obtain the new network behavior during faults. Then, it is possible to study the possible effects of DPOM on the operation of protective devices.

Chapter 3

Challenges of over-current protection during DPOM

In this chapter, the challenges caused by DPOM on the operation of phase and earth over-current relays will be discussed. Case studies will be presented to show that the settings and methodologies for coordinating the relays during TPOM are not applicable during DPOM. To this aim, the test system of this project is introduced first. Then a review of over-current relays is presented. Afterward, coordination methodologies applied to these relays are explained. later on, different scenarios of DPOM are applied to a test system, and challenges caused by DPOM on the operation of over-current relays will be revealed. Finally, the proposed solution for these challenges will be presented.

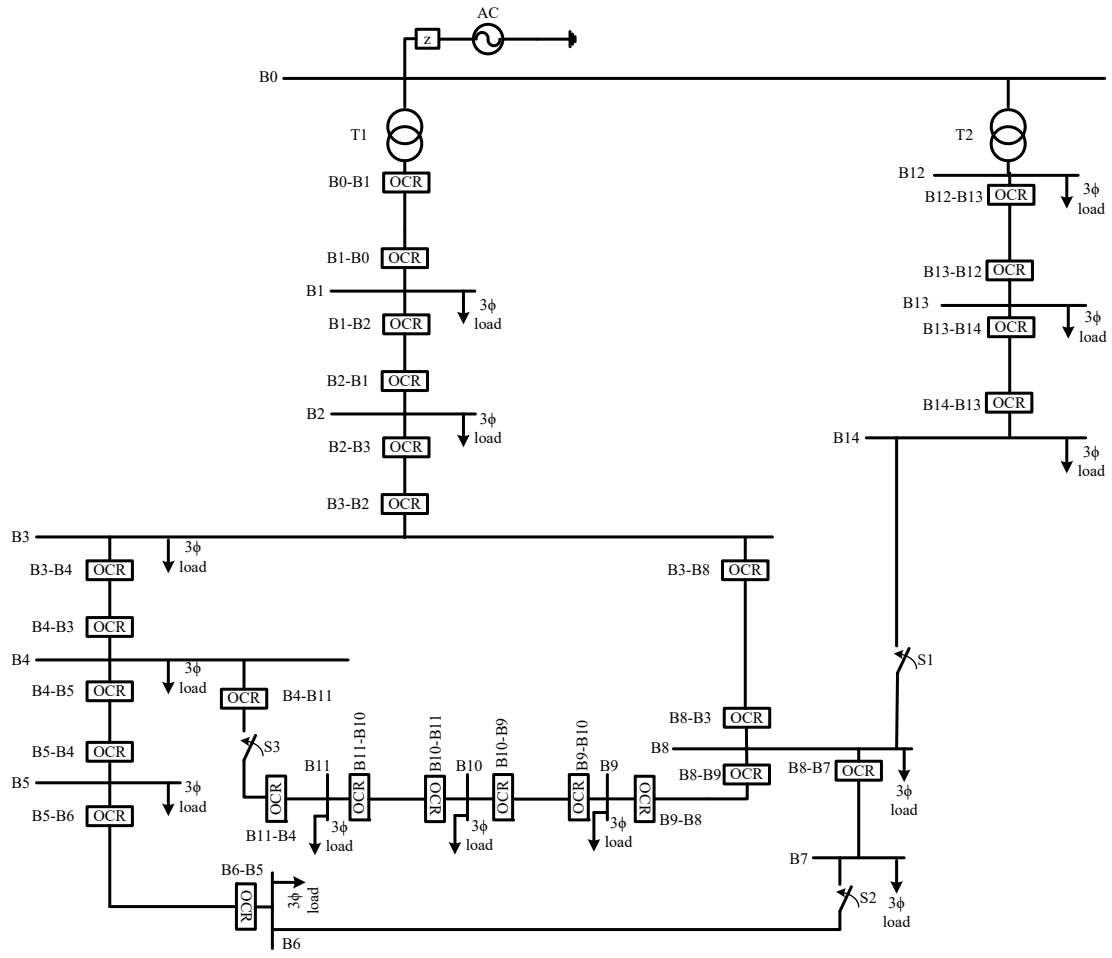

Figure 3.1: Single-line diagram of project test system.

3.1 Test system

This study focuses on grounded distribution systems, which are the most common type of distribution systems in North America. For this purpose, the North-American version of the CIGRE medium-voltage (MV) benchmark system is modeled using PSCAD/EMTDC program [12]. Figure 3.1 shows the single-line diagram of CIGRE MV distribution system benchmark.

3.1.1 Structure of the test system

The North American MV distribution feeders can have both radial and meshed structures. The former is more common and the latter is more used in rural installations. In North America, the radial structure is widespread, and thus single-phase MV laterals emanate from three-phase main feeders.

As shown in Figure 3.1, the left side feeder of the North American distribution network is connected to the main network through a 115kV/12.47kV transformer. Hence, the voltage on three-phase sections is 12.47 kV, and on the single-phase sections, the line-to-neutral voltage is 7.2kV. The nominal frequency is 60Hz. Based on [12], this feeder is suitable for various studies, including grid integration of DG units and distribution protection studies. Furthermore, the presence of three switches, S1, S2, and S3, as shown in figure 3.1, can create 8 new configurations for the network.

As shown in Figure 3.1, switch S1 is located between bus B14 and bus B8. By closing switch S1, bus B14 is connected to bus B8 and creates a loop starting from bus B0 to buses B1, B2, B3, B8, B14, B13, B12 and returns back to bus B0. This loop connects the left feeder to the right feeder. The other switch, S2, is located between bus B6 and B7 in Figure 3.1. Closing switch S2 results in creating a loop starting from bus B3 to buses B8, B7, B6, B5, B4 and returning back to bus B3. The last available switch on this network shown in figure 3.1 is switch S3, located between bus B4 and bus B11. Closed mode of this switch results in connecting bus B4 to bus B11 and creates a loop in the system starting from bus B3 to buses B4, B11, B10, B9, B8 and ends up by returning to

bus B3. More different network configurations can be achieved by changing the status of more than one switch in the network at the same time. In total, 8 different network configuration can be achieved by changing the status of these switches. In this project, the status of switch S3 is changed from the open mode to close mode when a loop is needed to be created in the network.

3.1.2 Test system parameters

Table 3.1 provides the positive and zero-sequence resistance, reactance and susceptance values of the lines.

Table 3.1: Connections and line parameters for three-phase laterals of the test system.

Line Segment	Node From	Node to	Conductor	R'_{Ph} ($\frac{Ohm}{km}$)	X'_{Ph} ($\frac{Ohm}{km}$)	B'_{Ph} ($\frac{\mu S}{km}$)	R'_{o} ($\frac{Ohm}{m}$)	X'_{o} ($\frac{Ohm}{m}$)	B'_{o} ($\frac{\mu S}{m}$)	Length (km)
1	1	2	1	0.173	0.432	3.83	0.351	1.8	1.57	1.2
2	2	3	1	0.173	0.432	3.83	0.351	1.8	1.57	1
3	3	4	1	0.173	0.432	3.83	0.351	1.8	1.57	0.61
4	4	5	1	0.173	0.432	3.83	0.351	1.8	1.57	0.56
5	5	6	1	0.173	0.432	3.83	0.351	1.8	1.57	1.54
6	6	7	1	0.173	0.432	3.83	0.351	1.8	1.57	0.24
7	7	8	1	0.173	0.432	3.83	0.351	1.8	1.57	1.67
8	8	9	1	0.173	0.432	3.83	0.351	1.8	1.57	0.32
9	9	10	1	0.173	0.432	3.83	0.351	1.8	1.57	0.77
10	10	11	1	0.173	0.432	3.83	0.351	1.8	1.57	0.33
11	11	4	1	0.173	0.432	3.83	0.351	1.8	1.57	0.49
12	3	8	1	0.173	0.432	3.83	0.351	1.8	1.57	1.3
13	12	13	1	0.173	0.432	3.83	0.351	1.8	1.57	4.89
14	13	14	1	0.173	0.432	3.83	0.351	1.8	1.57	2.99
15	14	8	1	0.173	0.432	3.83	0.351	1.8	1.57	2

Table 3.2: Transformer parameters for the test system.

Transformer	Node From	Node To	Connection	V_1 (kV)	V_2 (kV)	Z_{tr} (Ω)	S_{rated} (MVA)
T1	0	1	3ph D-Y HV and LV sides Grounded	115	12.47	0.010 + j1.24	15/20/25
T2	0	12	3ph D-Y HV and LV sides Grounded	115	12.47	0.013 + j1.55	12/16/20

Table 3.2 tabulates the transformers parameters. The more common transformer winding connection in North American networks is Delta and grounded Wye (Dyg). According to the cooling system of the transformer, three different values for the rated power of the transformers can be obtained. The first, second and third numbers in the last column of table 3.2 represent the nominal rate for transformers T1 and T2 considering natural cooling, single-fan cooling, and dual-fan cooling, respectively. The impedances are given based on the lowest MVA rating and referred to the low voltage side.

Table 3.3 shows the load data of the network. In this table Com, Res, Ind and PF stand for commercial, residential, industrial and power factor, respectively. Each phase supplies residential, commercial or industrial loads with different PFs. Based on [12], the single-phase subnetworks can be modeled with an equivalent load of 172 KVA.

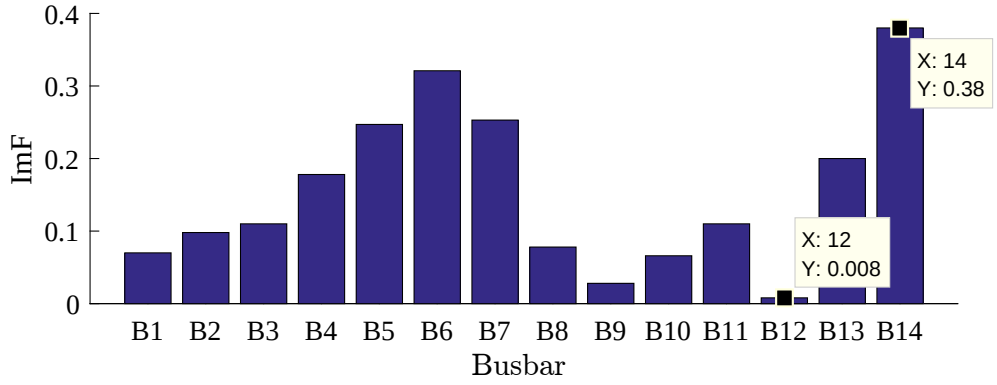

Figure 3.2: Imbalance factor of the test system busbars.

The loads that are connected to each phase are not balanced, as is normally the case for an actual distribution system. Imbalance factor is a parameter that shows the amount of load imbalance at each bus and is calculated using equation (3.1).

$$ImF = \frac{I^{-}}{I^{+}} \tag{3.1}$$

In equation (3.1), I^{-} and I^{+} are negative-sequence and positive sequence current flowing through each bus, respectively. Figure 3.2 depicts a histogram of the imbalance factor for each bus. As shown in figure 3.2, the maximum and minimum imbalance factors are for bus B14 and bus B12, respectively. At the right side feeder, bus B6 and bus B9 have the maximum and minimum imbalance factors, respectively.

Table 3.3: Load data of the MV distribution system benchmark.

Bus	Ph A Residential (KVA)	Ph A Com/Ind (KVA)	Ph B Residential (KVA)	Ph B Com/Ind (KVA)	Ph C Res (KVA)	Ph C Com/Ind (KVA)	P.F Res	PF Com/Ind
B1	172	—	—	100	200	100	0.90	0.80
B2	100	200	50	200	—	200	0.95	0.85
B3	0	80	200	80	50	80	0.90	0.80
B4	200	—	100	—	100	—	0.90	—
B5	200	50	172	200	—	50	0.95	0.85
B6	50	—	100	—	172	—	0.95	—
B7	—	100	100	100	—	100	0.95	0.95
B8	100	—	150	—	—	200	0.90	0.90
B9	100	—	150	—	100	—	0.95	—
B10	150	—	100	—	250	—	0.90	—
B11	50	150	50	150	—	150	0.95	0.85
B12	172	80	172	80	—	80	0.90	0.80
B13	—	145	—	145	—	145	0.95	0.85
B14	—	90	—	90	172	90	0.90	0.90

3.2 Phase over-current relays

Time-inverse over-current relaying is one of the earliest and most common methods of distribution system protection [13][14][15]. The design of these relays used to be based on an induction disk [16], which operated based on the magnitude of the current measured by the relay. The larger the current is, the faster the trip signal is issued. This behavior results in an inverse-time characteristic for the relays. Similar behavior is emulated by digital over-current relays. Based on the IEEE standard for inverse-time over-current relay [17], a digital inverse-time over-current relay is a current-operated relay that represents an inverse time-current characteristic similar to that of an induction disk. Equation (3.2) shows the mathematical relation between operation

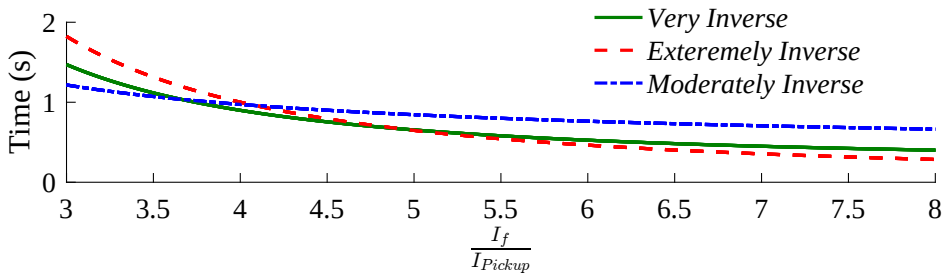

Figure 3.3: Different types of OC inverse time−current relays.

time and the current flowing through the relay.

$$t(I) = TDS.(\frac{A}{(\frac{I_f}{I_{pickup}})^p - 1} + B) \tag{3.2}$$

In equation (3.2), I_{pickup} is the pickup setting of the relay. The pickup setting is the current above which the relay starts operating. In equation (3.2), A,B and p are the constant numbers. Based on the values of these constants different inverse time-current characteristics are obtained for the relays. These different characteristics are moderately inverse (MI), very inverse (VI) and extremely inverse (EI) over-current relays. Table 3.4 shows the standard values for A,B and p for different types of the over-current relays based on [17]. The time-current characteristic of MI, VI and EI over-current relays are depicted in figure 3.3.

Each of these relays is suitable for specific circumstances. For instance, VI over-current relays are used for feeders where the fault current reduces significantly in downstream buses. EI relays, on the other hand, are suitable for coordination with fuses, and MIs are used when the maximum fault current is not much higher than the maximum load current.

Digital microprocessor-based relays are equipped with logical circuits, metering functions

Table 3.4: Moderately inverse, very inverse and extremely inverse over-current relay constant numbers.

Characteristic	A	B	p
Moderately Inverse	0.0515	0.114	0.02
Very Inverse	19.61	0.491	2.00
Extremely Inverse	28.2	0.1217	2.00

and sometimes communication features. These features make the relays able to transfer the necessary information to other relays or to the utility information centers. These features provide protection engineers the ability to make changes on the characteristics or settings of the relays during specific operating conditions like DPOM[18][19][20][21][22][23]. To coordinate the over-current relays the following process should be taken.

Over-current relays have two setting parameters that are necessary to be tuned precisely to guarantee proper operation of relays at fault situations [16][17][24][25].

- **Pickup current**

  The pickup current is the current at which the relay starts to operate. An appropriate setting for pickup current is the value at which the relay does not trip for the maximum load current, fast overshoots in load current, or transformer inrush current. This setting should also be smaller than minimum fault current, magnitude, so no fault remains undetected. Based on [17], a factor of 1.2 to 1.5 usually can provide a proper pickup setting

based on the aforementioned criteria.

- **Time Dial Setting (TDS)**

  The other setting of over-current relays is TDS. TDS setting is used for operation time coordination of main and backup relays for each line. By increasing the value of TDS, the operation time of the relay increases for each fault current. This would accordingly increase the usable time margin for backup protection.

In order to find the appropriate setting for the relays, a coordination process should be performed for the relays of the network. Figure 3.4 illustrates the conventional coordination process of over-current relays. In this figure, j is the relay order number (RON) in the system. A, B and p are constants that identify the inverse time-current characteristic of the relay. I_F is the maximum fault current by the downstream relay. I_{Pic} is the pickup current, which is 1.5 times the maximum load current in this study to guarantee enough margin between the possible overshoots of load currents in the test system and minimum fault current of the test system network.

Considering the sample network given in figure 3.5, time coordination process starts from the fastest relay-most downstream relay- which is relay R1 in this figure. TDS for this relay is minimum which is 0.5. To find the TDS of the upstream relay, R2, the operation time of the relay R1 for the maximum fault current at the same bus, bus B4 in figure 3.5 should be calculated. The maximum fault current is considered as a bolted three-phase-to-ground fault on the bus B4. Then the operation time for the relay R2 for the same value of fault current is shifted up by a time

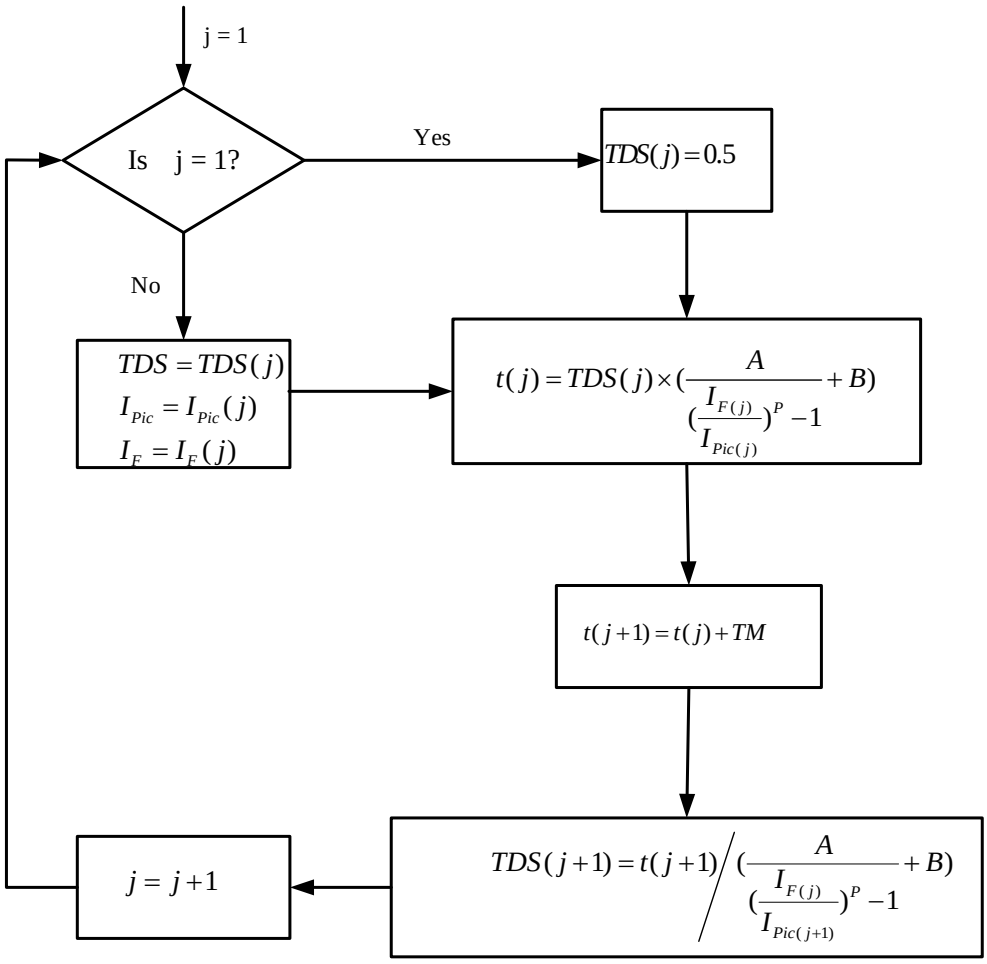

Figure 3.4: Over-current relays coordination process.

margin (TM). The final step is to calculate the TDS of the relay R2 and this process goes on to get the TDS of last relay.

To illustrate more on the coordination process, a coordination example is provided for the basic distribution feeder in figure 3.5. The load current values are given in figure 3.5 and table 3.5 tabulates the relays settings for this network. As shown in table 3.5, relay R1 is the fastest relay since it is the most downstream relay in the network. The settings for the other relays are

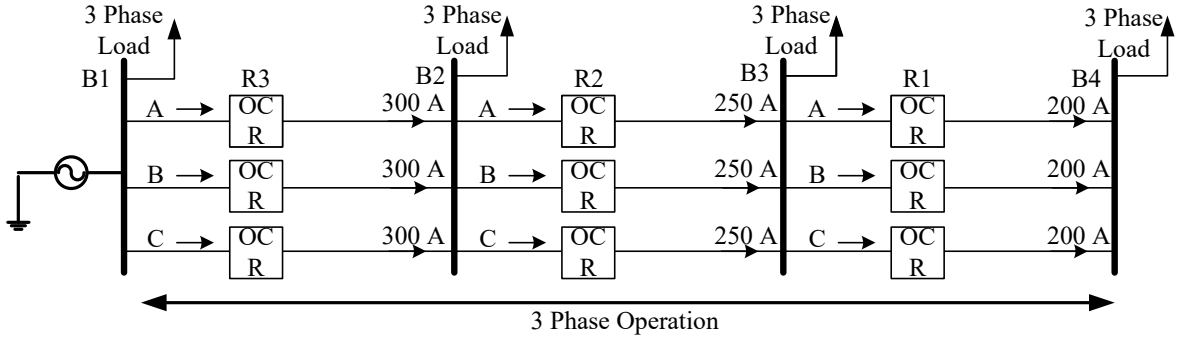

Figure 3.5: Diagram of a sample power network operating in three-phase mode.

Table 3.5: Phase relay settings during three phase operation mode.

Relay	$I_{F_{3\phi}}$Max (A)	I_{pickup} (A)	TDS
R1	5000	360	1.1
R2	3000	300	0.7
R3	1500	240	0.5

obtained based on the coordination process depicted in figure 3.4.

3.3 Phase over-current protection during DPOM

This section presents the investigation of the operation of phase over-current relays during DPOM. Using the following parameters, the appropriate setting for the phase over-current relays are obtained.

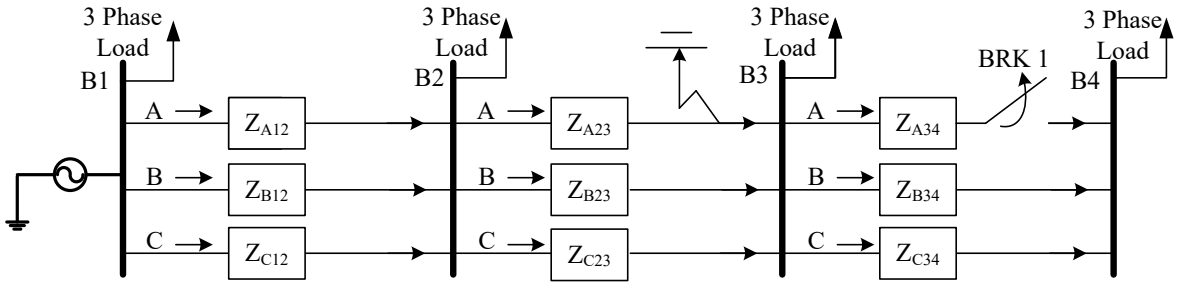

Figure 3.6: Maximum fault current calculation during TPOM and DPOM.

- **Load current**

  The current through each phase during normal operation of the network plays a critical role in choosing the pickup setting of over-current relays. During DPOM, due to the reduction in the amount of the load connected to the network, the load current flowing through each phase decreases and thus, the old pickup settings are no longer valid. The load current, and so the pick-up setting, also indirectly affects the TDS setting.

- **Maximum fault current during DPOM**

  Another parameter that impacts the TDS setting of the phase over-current relays is the maximum fault current measured by each relay. This parameter during DPOM is the same as that of TPOM, since the phase impedance between the generation units and fault point is constant and independent of one or two phase being out of service. Take, for instance, the system in figure 3.6. Maximum phase fault current of phase A on bus B3 in the system of figure 3.6 is calculated using equation (3.3).

$$I_{F_A} = \frac{V_A}{3.(Z_{A12} + Z_{A23})} \tag{3.3}$$

In equation (3.3), Z_{A12} and Z_{A23} are the phase impedance of the feeders between buses B1 and B2 and B2 and B3, respectively, and V_A represents the voltage of phase A at bus B3. As shown in figure 3.6 and equation (3.3), the operation of breaker BRK1 does not affect I_{F_A}.

Analyzing the effects of DPOM on the operation of the relays initially requires load flow and fault analysis for the systems during DPOM and finding the settings of the relays during this period. For example, consider the original system shown in figure 3.5 which includes the load current flowing through each phase of the network. The results of network analysis along with the relay settings are tabulated in table 3.5. After phase A is opened between buses B3 and B4 in figure 3.5, the system will operate partly in DPOM and partly in TPOM. Figure 3.7 shows the new network operation during DPOM. As it is portrayed in this figure, the current flowing through phase A of the system between bus B1 to B2 and B2 to B3 is different from that of TPOM. Hence, the relay settings for phase A during TPOM of relays B1-B2 and B2-B3 are not valid for DPOM. By performing a coordination analysis on the network during DPOM, the new relay settings, shown in table 3.6, are obtained.

By comparing the phase load current during DPOM and TPOM, a significant reduction is monitored, which necessitates resetting the pickup settings of the relays. Furthermore, the order of the relays is different during DPOM. For instance, during TPOM, relay B3-B4 is the most downstream relay, thus, it is the fastest relay with TDS of 0.5. However, during DPOM, there is no

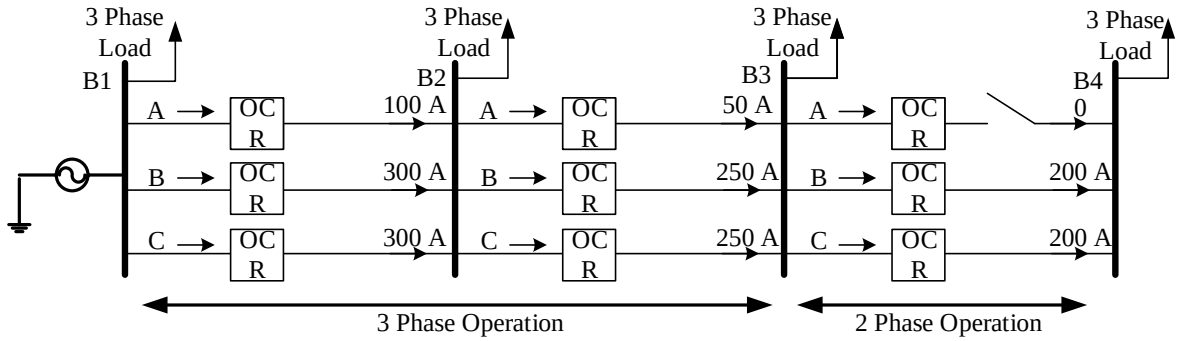

Figure 3.7: Diagram of a sample distribution feeder operating in double phase mode.

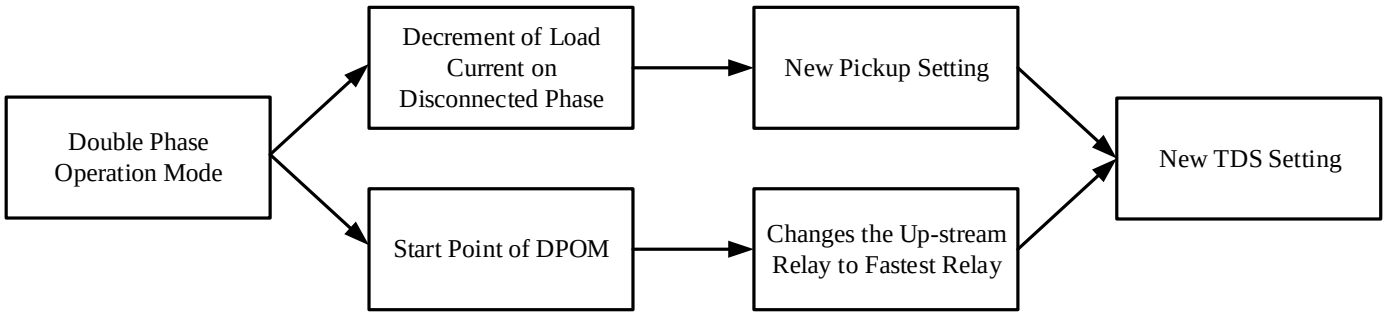

Figure 3.8: Double phase operation mode effects on the phase relay settings.

relay B3-B4 for phase A of the system. This means that relay B2-B3 on phase A is the fastest relay and the TDS is 0.5. Figure 3.8 depicts the changes in the network during DPOM that result in the necessity of re-coordination of the protective devices during DPOM.

3.3.1 Case studies

For more clarifications on the changes caused by DPOM on the network, different scenarios of DPOM are investigated for the CIGRE distribution benchmark system depicted in figure 3.1.

Table 3.6: Phase relay settings for the disconnected phase (A). Double phase operation mode starts from Bus B3.

Relay	$I_{F_{3\phi}}$Max (A)	I_{pickup} (A)	TDS
B1-B2	5000	120	1.5
B2-B3	3000	60	0.5
B3-B4	NA	NA	NA

These scenarios are categorized into two different groups based on the network structure and whether or not DG units are connected to the network.

Radial network without DG units

As the first scenario, suppose that switch S3 in figure 3.1 is open and DPOM starts from the line between Bus B3 and B4 by disconnecting phase A from the system. Hence, the system from Bus B4 to Bus B6 operates in DPOM. Table 3.7 tabulates the fault analysis data of the network for disconnected phase A. Furthermore, the new relay setting during DPOM are presented in table 3.7. The currents are given in kA. As it is expected, since the loads on phase A are disconnected from bus B3, the total load current flowing through the upstream of phase A relays decreases. Hence, as illustrated in figure 3.8, new TDS settings should be derived for the relays of the

Table 3.7: Disconnected phase (A) current analysis data during DPOM starting from Bus B4. Switch S3 is open and no DG is connected to the network.

Relay	$I_{\phi A_{3\phi}}$ (kA)	$I_{\phi A_{2\phi}}$ (kA)	Old I_{Pickup} (kA)	New I_{Pickup} (kA)	Old TDS	New TDS
B0-B1	0.246	0.176	0.295	0.21	4.3	3.6
B1-B2	0.221	0.151	0.265	0.18	2.9	3.2
B2-B3	0.177	0.107	0.21	0.12	2.3	2.7
B3-B8	0.094	0.094	0.113	0.113	1.9	1.9
B8-B9	0.065	0.065	0.08	0.08	1.6	1.6
B9-B10	0.05	0.05	0.06	0.06	1.1	1.1
B10-B11	0.03	0.03	0.035	0.035	0.5	0.5

network.

Radial network with type 4 DG units

This scenario studies the effects of DPOM on the operation of phase over-current relays when an inverter-based DG unit, such as a Type 4 wind unit, is connected to the network. A 5 MVA type 4 wind turbine unit is modeled in PSCAD/EMTDC. Table 3.8 shows the parameters of this unit.

Table 3.8: Type 4 wind turbine parameters

Converter Reactor (H)	Capacitance (mF)	Machine Frequency (Hz)	AC system Frequency (Hz)	Machine Terminal Voltage (kV)	Stator Resistance (p.u.)	System MVA
0.000135	40	30	60	0.69	0.0054	5

In this scenario, switch S3 in figure 3.1 remains open to keep the configuration of the network radial. The type 4 wind turbine is connected to bus B3, and DPOM starts from Bus B8. The results of the network analysis for this scenario as well as the DPOM settings for the relays are given in table 3.9. In table 3.9, load current for phase A during TPOM and DPOM is given in the second and third columns, respectively. For the relays B0-B1, B1-B2 and B2-B3 there is an increase in the amount of the current flowing through these relays. The reason for this increase is that the load that the load connected to phase A of bus B8, B9, B10, and B11 are disconnected from the grid. This disconnection results in a decrement in the load that was supplied by the wind turbine. On the other hand, the DG unit has a constant generation during DPOM and TPOM. Hence, the power generated by the wind turbine is injected to the main grid, through buses B3, B2, B1, and B0. This means the flowing current through these feeders increases. This increase in the amount of phase current can cause false trips of the relays, and thus, it is vital in this case to re-coordinate the relays. The valid settings for the relays during DPOM is given in table 3.9. During DPOM, relay B8-B7 in figure 3.1 is considered as the most downstream relay, and thus has the minimum TDS. Other relays are coordinated based on the methodology presented in

Table 3.9: Disconnected phase (A) current analysis data during DPOM starting from Bus B8. Switch S3 is open and a type 4 wind turbine is connected to bus B3.

Relay	$I_{\phi A_{3\phi}}$ (kA)	$I_{\phi A_{2\phi}}$ (kA)	Old I_{Pickup} (kA)	New I_{Pickup} (kA)	Old TDS	New TDS
B0-B1	0.085	0.091	0.102	0.11	4.3	3.7
B1-B2	0.085	0.1	0.102	0.12	2.9	2.8
B2-B3	0.093	0.125	0.11	0.15	2.3	2.1
B3-B8	0.096	0.03	0.115	0.036	1.9	1.1
B8-B7	0.015	0.015	0.018	0.018	0.5	0.5

section 3.2. By comparing the new TDS and old TDS settings, the necessity of re-coordination of the relays during DPOM is clear.

Meshed network with type 4 wind DG units

In this scenario, switch S3 in figure 3.1 is closed to connect bus B4 to bus B11 and make a loop starting from bus B3 to buses B8, B9, B10, B11, B4 and returns back to bus B3. The type 4 wind turbine is connected to bus B3, and DPOM starts from Bus B8. The results of the network analysis for this scenario as well as the DPOM settings for the relays are given in table 3.10. In table 3.10, load current for phase A during TPOM and DPOM is given in the second and third columns,

Table 3.10: Disconnected phase (A) current analysis data during DPOM starting from Bus B8. Switch S3 is closed and a type 4 wind turbine is connected to bus B3.

Relay	$I_{\phi A_{3\phi}}$ (kA)	$I_{\phi A_{2\phi}}$ (kA)	Old I_{Pickup} (kA)	New I_{Pickup} (kA)	Old TDS	New TDS
B3-B4	0.1	0.14	0.13	0.17	1.6	1.8
B4-B11	0.027	0.06	0.036	0.08	3.4	1.7
B11-B10	0.02	0.03	0.024	0.04	2.8	1.1
B10-B9	0.024	0.015	0.03	0.02	2.1	0.5

respectively. For the relays B3-B4, B4-B11 and B11-B10 and B10-B9 there is an increase in the amount of the current flowing through these relays. The reason for this increase is that during TPOM, the loads connected to phase A of buses B8, B9, B10, and B11 were supplied through feeder B3-B8 and B4-B11. During DPOM, however, loads connected to buses B8, B9, B10 and B11 are supplied only through feeder B4-B11. This leads to increase in the amount of the current flowing through this feeder. This increase in the amount of phase current can cause false trips of the relays, and thus, it is vital in this case to re-coordinate the relays. The valid settings for the relays during DPOM is given in table 3.10. During DPOM, relay B10-B9 in figure 3.1 is considered as the most downstream relay, and thus has the minimum TDS. Other relays are coordinated based on the methodology presented in section 3.2. By comparing the new TDS and old TDS settings, the necessity of re-coordination of the relays during DPOM is clear.

3.4 Earth-fault over-current relays

Earth-fault relays protect the system generally from the single-phase-to-ground faults by measuring the zero-sequence current flowing through the relay. Zero-sequence current flows through the system as a result of the unbalanced loads connected to each phase of the system. Since the amount of zero-sequence current is considerably lower than phases load current, the pickup setting for earth-fault relays can be set very lower than pickup setting for phase relays. This feature gives a high sensibility to the earth-fault relays. The pickup setting for earth-fault relays is usually picked as 10 to 15 percent of the maximum phase load current[4][5]. It should be mentioned that coordination process of earth-fault relays is the same as of the phase relays. The only difference is the measured element with the relay which is the zero-sequence current. Hence, the coordination process explained in section 3.2 is used for earth-fault relays as well.

3.5 Earth-fault over-current protection during DPOM

Despite TPOM, during DPOM, the normal zero-sequence current of the network increases due to the noticeable unbalanced load connected to the disconnected phase of the system. Thus, malfunction of the earth-fault relays is very likely to happen. To elaborate more on this issue, consider the same scenario applied to the network depicted in figure 3.5 and figure 3.7 during TPOM and DPOM, respectively. As shown in figure 3.7, there is a noticeable unbalanced load current flowing through the phases which causes an increase in the amount of the normal zero-

sequence current flowing through the earth-fault relay during DPOM. For instance, let's calculate the normal zero-sequence current flowing through relay B3-B4 during TPOM and DPOM.

$$3I_o = I_A + I_B + I_C = 200\angle 0^\circ + 200\angle -120^\circ + 200\angle +120^\circ = 0 \tag{3.4}$$

Equation (3.4) shows the normal zero-sequence current flowing through earth-fault element of relay B3-B4 during TPOM. Equation (3.5) calculates the normal operation zero-sequence current flowing through the same relay during DPOM using figure (3.7).

$$3I_o = I_A + I_B + I_C = 0 + 200\angle -120^\circ + 200\angle +120^\circ = 200\angle 180^\circ \tag{3.5}$$

Based on the conventional coordination method for earth-fault relays, the pickup setting for the earth-fault relay B3-B4 is calculated in equation (3.6).

$$I_{Pickup} = 0.1.I_{PhaseA} = 0.1 \times 200 = 20A \tag{3.6}$$

Comparing the normal zero-sequence current flowing through relay B3-B4 during DPOM given in equation (3.5) and pickup setting of this relay given in equation (3.6), the malfunction of the earth-fault relay is certain. Figure 3.9 depicts the changes on the network during DPOM that result in necessity of re-coordination of earth-fault relays during DPOM.

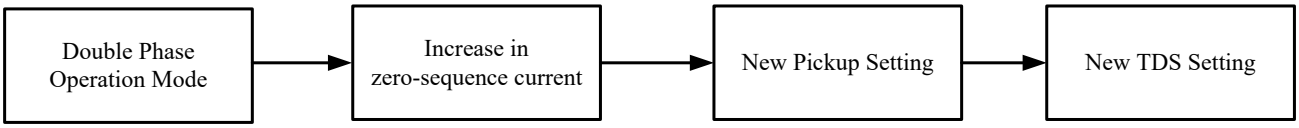

Figure 3.9: Double phase operation mode effects on the earth-fault relay settings.

3.5.1 Case studies

In this section, case studies are presented to elaborate more the challenges caused by DPOM on earth-fault relays. The scenarios for studying the operation of earth-fault relays is same as of that applied for phase relays, presented in section 3.3.1. For the sake of reviewing the scenarios, a summary of the scenarios are applied to the test system is presented here.

Radial network without DG unit

As the first scenario, suppose that switch S3 in figure 3.1 is open and DPOM starts from the line between Bus B3 and B4 by disconnecting phase A from the system. Hence, the system from Bus B4 to Bus B6 operates in DPOM. Table 3.11 tabulates the zero-sequence current analysis of the network. Furthermore, the new relay settings during DPOM are presented in table 3.7. Table 3.11 shows the zero-sequence current analysis of the network and compares it with the data of the network during TPOM. The second and third column of table 3.11 shows the normal zero-sequence current flowing through the relays during TPOM and DPOM, respectively. This data shows that the zero-sequence current during DPOM increases and thus, the old pickup settings are not valid and can cause malfunction of the relays. This can be concluded by comparing

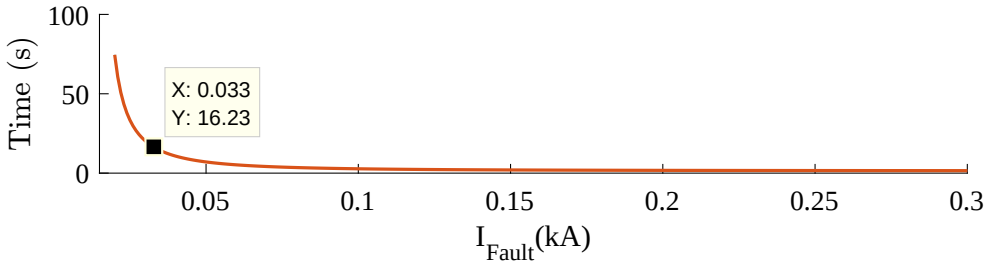

Figure 3.10: t-I curve of relay B1-B2 with old pickup settings.

the $I^o_{2\phi}$ and old I^o_{pickup}. For instance, consider relay B1-B2. The zero-sequence current during DPOM is 33 A while the old pickup setting for this relay set to 15 A. This will result in a false trip of this relay during DPOM. Figure 3.10 depicts the t-I curve of relay B1-B2 and shows the operation time of this relay for 33 A zero-sequence current. Based on figure 3.10, relay B1-B2 will operate in 16.23 second after the beginning of DPOM.

Increasing the pickup setting indirectly affects the TDS setting and thus, the old TDS values are no longer valid. By re-coordinating the relays during DPOM, new settings for the earth-fault relays will be obtained which are tabulated in table 3.11.

Meshed network with type 4 wind DG units

In this scenario, switch S3 in figure 3.1 is closed to connect bus B4 to bus B11 and make a loop starting from bus B3 to buses B8, B9, B10, B11, B4 and returns back to bus B3. The type 4 wind turbine is connected to bus B3, and DPOM starts from Bus B8. The results of the network analysis for this scenario as well as the DPOM settings for the relays are given in table 3.12. In table 3.12,

Table 3.11: Zero-sequence current analysis for DPOM starts from Bus B3 and earth-fault relay settings during TPOM and DPOM. System is in radial configuration and no DG unit is connected.

Relay	$I^{o}_{3\phi}$ (kA)	$I^{o}_{2\phi}$ (kA)	Old I^{o}_{Pickup} (kA)	New I^{o}_{Pickup} (kA)	Old TDS	New TDS
B0-B1	0.010	0.031	0.013	0.036	3.5	4.1
B1-B2	0.018	0.033	0.015	0.04	2.9	3.4
B2-B3	0.019	0.037	0.03	0.04	2.3	2.6
B3-B4	0.009	0.024	0.018	0.03	1.6	1.7
B4-B5	0.010	0.02	0.015	0.024	1.1	1.1
B5-B6	0.005	0.007	0.015	0.0084	0.5	0.5
B3-B8	0.007	0.006	0.014	0.007	2.1	2.3
B8-B9	0.002	0.003	0.014	0.004	1.7	1.7
B9-B10	0.004	0.009	0.012	0.011	1.1	1.1
B10-B11	0.002	0.002	0.035	0.003	0.5	0.5

load current for phase A during TPOM and DPOM is given in the second and third columns, respectively. Despite other scenarios that DPOM has direct effect on the operation of earth-fault relays, this scenario, as shown in table 3.12, does not have a significant effect on the operation of these relays. The reason is the presence of the DG unit and the meshed configuration of the network. These two elements provide a rigid configuration to the network. When breaker between bus B3 and B8 operates, loads connected to phase A of buses B8, B9, B10, B11, and B4 are not supplied by feeder B3-B8. However, these loads are supplied with feeder B3-B4 which supports the system to operate normally.

Table 3.12: Zero-sequence current analysis for DPOM starting from Bus B8 and earth-fault relay settings during TPOM and DPOM. System has meshed configuration and DG unit is connected to bus B3.

Relay	$I^o_{3\phi}$ (kA)	$I^o_{2\phi}$ (kA)	Old I^o_{Pickup} (kA)	New I^o_{Pickup} (kA)	Old TDS	New TDS
B0-B1	0.005	0.005	0.006	0.006	3.5	3.5
B1-B2	0.014	0.014	0.017	0.017	2.9	2.9
B2-B3	0.014	0.014	0.017	0.017	2.3	2.3
B3-B4	0.007	0.009	0.009	0.011	1.7	1.7
B4-B5	0.01	0.010	0.012	0.012	1.1	1.1
B5-B6	0.005	0.005	0.006	0.006	0.5	0.5
B3-B8	0.006	0.01	0.007	0.013	3.8	3.8
B8-B9	0.001	0.003	0.003	0.004	3.2	3.2
B9-B10	0.002	0.003	0.003	0.004	2.5	2.5
B10-B11	0.006	0.003	0.008	0.005	1.8	1.8
B11-B4	0.003	0.003	0.004	0.004	1.2	1.2
B4-B3	0.007	0.009	0.009	0.011	0.5	0.5
B3-B2	0.014	0.015	0.017	0.017	1.5	1.5
B2-B1	0.014	0.014	0.017	0.017	0.9	0.9
B1-B0	0.005	0.005	0.006	0.006	0.5	0.5

3.6 Conclusion

In this chapter, the changes caused by DPOM on the operation of protective devices, i.e, phase over current and earth-fault over-current relays were discussed. Following concludes the changes

caused by DPOM on these two most-common protective devices in distribution networks.

- **Phase over-current relays**
  - **Change in current flowing through the relay**

    DPOM changes the configuration of the network and this leads to a change in the current flowing through the relays. This change necessitates change in the pickup setting of the relays.
  - **Change in the RON**

    Relay order number changes due to the operation of the breakers. This has direct effect on the TDS setting of phase over-current relays.

  The aforementioned reasons cause malfunction of the phase over-current relays during DPOM and necessitates the re-coordination of the relays.

- **Earth-fault over-current relays**
  - **Change in zero-sequence current**

    Zero-sequence current flowing through earth-fault relays changes as the result of DPOM. DPOM causes unbalanced load on the buses which leads to increment in the level of zero-sequence current. Malfunction of this type of relay is very likely during DPOM.

By understanding the changes caused by DPOM on the operation of these relays, finding a new

methodology for re-coordination of the relays during DPOM will be the next step of this project which is presented in next chapter.

Chapter 4

Re-coordination of over-current relays for DPOM

In chapter 3, the changes caused by DPOM on the distribution network were presented. The mentioned changes causes challenges on operation of the protective devices which were also discussed in chapter 3. Based on these studies, re-coordination of the over-current relays during DPOM is a critical action should be taken as soon as DPOM starts. In this chapter, a new methodology for re-coordination of the over-current relays is presented. Afterward, the methodology is evaluated by applying it on protective relays of the project test system.

4.1 Proposed solution

To re-coordinate the over-current relays during DPOM, a methodology should be provided that promptly obtains new settings for the relays based on the new network parameters. Two critical factors must be considered in this methodology:

- **Benefiting from local measurement**

  Local measurement is referred to the parameters that a relay measures. These parameters include load current, sequence currents, busbar voltage and so on. The main parameter that is used for coordination of phase or zero-sequence over-current relays is the load current and zero-sequence currents, respectively. By benefiting from locally measured network parameters, the necessary information for setting the relays during DPOM is provided.

- **Fast and reliable**

  It is vital to have the relays coordinated as soon as DPOM starts. Otherwise, the system will be left unprotected. Hence, the provided solution for re-coordination of the relays should be fast to guarantee the protection of the system.

To achieve the new settings based on the aforementioned factors, two sets of settings is proposed to be applied to the relays during DPOM.

- **Prompt settings**

To ensure that the protective relays are capable of protecting the system as soon as DPOM starts, a prompt setting should be obtained by the relay based on the local measurements and the DPOM start location. Prompt settings are the temporary settings that are available on the relays until the optimum settings are obtained and updated on all the relays of the network.

- **Optimum settings**

  By applying the prompt settings on the relays of the network, the protection of the system is ensured, however, the prompt settings are not necessarily the optimum settings that could be applied on the relays. Optimum settings in this project refers to the settings that minimize the operation time of the relays in the system. These settings and the method of obtaining them will be clarified in details shortly.

4.2 Phase over-current relays

Following, presents the re-coordination process for phase over-current relays during DPOM. Prompt settings and optimum settings, as the two type of settings will be applied on phase over-current relays should a DPOM incident happens.

4.2.1 Prompt settings

Pickup current and TDS are the two setting variables that should be obtained to set the relays during DPOM. Pickup setting can be obtained by benefiting from the relays measurement independently from other relays of the network. Calculation of TDS, however, needs information from the downstream relays which takes longer time to obtain and needs a wide bandwidth communication facility. To cope with this issue, a new setting parameter is introduced called **PTDS**. PTDS or Prompt TDS is the new setting parameter that is obtained by local measurement and plays the role of TDS during DPOM. It should be mentioned that, these new settings are only applied on the upstream phase over-current relays which provide protection for the disconnected phase. For instance, consider the sample network presented in figure 3.7. In this network, phase A is disconnected from bus B3. The new settings will be applied only on the phase A of the upstream relays, B2-B3 and B1-B2. The phase over-current relays on healthy phases of the system benefit from the old settings. The methodology for obtaining the new pickup setting and PTDS during DPOM is presented in following.

- **Pickup current**

  By benefiting from the relays phase current measurements, pickup setting can be calculated by the microprocessor-based relays. The pickup setting will be calculated by multiplying the phase current with the old margin factor that was applied previously for calculating the pickup current.

- **PTDS**

TDS is a variable that is used for time-coordination of the relays with upstream and downstream relays. During DPOM, however, since a fast setting is needed to be applied on the relays, PTDS is introduced which plays the same role as of TDS. PTDS is obtained by benefiting from local measurement of the phase current. PTDS is calculated using equation (4.1).

$$PTDS = \frac{I_{L_{DPOM}}}{I_{L_{TPOM}}} \tag{4.1}$$

Where $I_{L_{DPOM}}$ and $I_{L_{TPOM}}$ are the disconnected phase load current during DPOM and the same phase load current during TPOM, respectively.

- **RON**

  RON shows the position of the relay with respect to the location of DPOM. Getting back to the sample network given in figure 3.7, RON of the relay B2-B3 during TPOM is 2. During DPOM, however, B2-B3 is the first over-current upstream relay from the DPOM start point. RON is used in the time-coordination of the relays during the period that prompt settings are applied on the relays. RON is obtained by receiving a low bandwidth communication signal from the operated breaker, communicated to the upstream relays to show the location of the DPOM start point. Based on that, relays calculate the RON. Equation (4.2) shows the calculation logic of the RON.

$$RON = RON_{TPOM} - OBON \tag{4.2}$$

  OBON in equation (4.2) is the operated breaker order number transferred to the upstream relays.

- **New t-I characteristic for prompt settings**

  Equation (4.3) shows the final t-I characteristic proposed for the phase over-current relays during the active prompt setting period of the over-current relays.

$$t(I) = PTDS.(\frac{A}{(\frac{I}{I_{pickup}})^{p} - 1} + B) + (RON - 1).TM \tag{4.3}$$

  Where TM is defined as the minimum time margin between operation of the main relay and backup relay. In this project, TM is considered to be 0.3 s. Figure 4.1 depicts the steps should be taken to obtain the prompt setting for the phase relays during DPOM.

4.2.2 Optimum settings

After applying the prompt settings on the relays for ensuring the protection of the system during DPOM, it is time for optimizing the relays operation time. To this aim, the local measurement data from each relay should be communicated to the Main Computing Data Center (MCDC) for performing the optimization process. It should be mentioned that, since an optimization process needs the complete network data, the communication between the relays and MCDC is unavoidable. This data include new load current for phase relays and relay's RON. The objective function of this optimization process is minimizing the operation time of the relays. The output of the optimization process is the TDS applied on the conventional t-I curve presented in equation (3.2). It is worth to mention that, in case of a failure in the communication between the MCDC and any relay, the prompt settings will be still applicable on the relays. Thus, not only do the prompt settings coordinate the relays instantly after the beginning of DPOM but

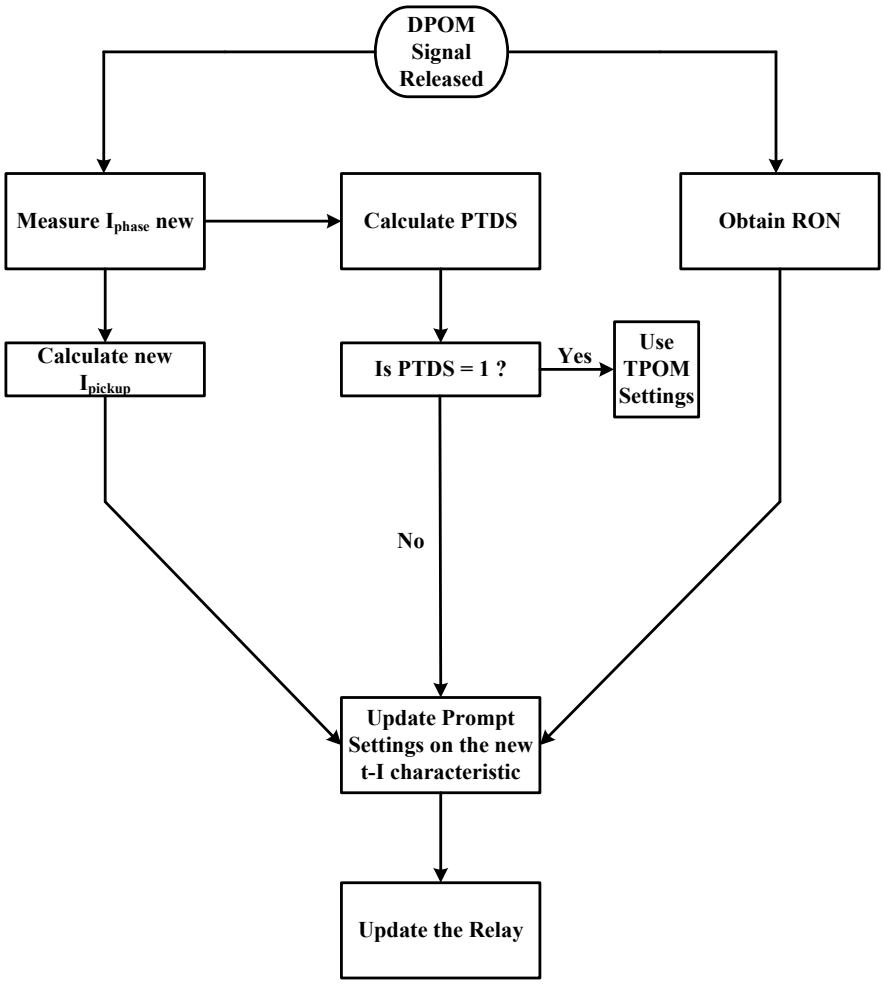

Figure 4.1: Prompt setting flowchart.

also it plays a backup role for optimum settings. For this purpose, among many optimization algorithm, Non Dominant Sorting Genetic Algorithm (NSGA II) is chosen [26]. This optimization algorithm finds the optimum solution by searching different regions in which the objective function is defined. Section 4.2.3 presents the relays coordination problem formulation which is the objective function of this project.

4.2.3 Protection coordination problem formulation

The protection coordination problem is developed to formulate the objective function of the optimization process [27]. The main objective of this function is to minimize the operation time of the relays in the system for different type of faults. This objective function is subject to constraints in regard with protection coordination, relay settings, and relay operating time. Equation (4.4) shows the objective function of this optimization problem.

$$T_{min} = \sum_{i=1}^{N} \sum_{j=1}^{M} \sum_{l=1}^{L} (t_{ijl}^{p} + \sum_{x=1}^{X} t^{b_{xijl_{ijl}}}) \tag{4.4}$$

In equation (4.4), N is the total number of relays. i is the relay identifier, M is the total number of fault types studied with j being the fault type identifier, and L is the total number of fault location investigated with l being the fault location identifier. The superscript p represents primary relays and b_{x} represents the backup relay x with X being the total number of backup relays for each primary relay. The backup relay x is dependent on the primary relay i for a fault type j that occurred at location l. The variables t_{ijl}^{p} and $t_{ijl}^{b_{xijl}}$ refer to the primary and backup relay i operating time for a fault of type j at location l, respectively.

The main output of this optimization process is the relay TDS setting. The pickup setting is a known parameter used from the relay measurement. It should be mentioned that this optimization problem is a linear problem since pickup setting is a constant number.

In this optimization problem, the model must satisfy the protection coordination constraints

which involves both linear and nonlinear constraints. In coordination process of the relays, each main relay should have a backup relay in case of a failure in tripping. Hence, a minimum time gap should be considered for operation of backup relay. This time gap is called Coordination Time Interval(CTI) which is considered to be 0.5 s in this project. The considered CTI in this project is the maximum recommended CTI by IEEE standard on over-current protection [17] that ensures that the optimization problem can maintain this constraint. Maintaining the CTI is one of the constraints of this optimization problem which is given in equation (4.5) .

$$t_{jl}^{b_x} - t_{jl}^{p} \geq CTI \quad \forall, \{l, x\}. \tag{4.5}$$

Two more constraints are applied on this optimization process to maintain the protection coordination conditions. The TDS of the relays is a parameter varying between $TDS_{i,min}$ and $TDS_{i,max}$ which are set to 0.5 and 10 in this project, respectively [17]. This constraint is formulated using equation (4.6).

$$TDS_{i,min} \leq TDS_i \leq TDS_{i,max} \quad \forall i \tag{4.6}$$

The last constraint for this optimization problem is the minimum operation time of the over-current relays. This lower limit is set to 20 ms in this project which is shown in equation (4.7) [16].

$$t^{p}_{ijl}, t^{b_x}_{ijl} \geq t_{ijl,min} \quad \forall i, j, \{l, x\} \tag{4.7}$$

The optimization process will be completed by using equation (4.4) and maintaining the constraints of this problem given in equations (4.5)-(4.7).

4.3 Earth-fault over-current relays

Following, presents the re-coordination process for earth-fault over-current relays during DPOM. Prompt settings and optimum settings, are the two type of settings which will be applied on phase over-current relays should a DPOM incident happens. Optimum settings for the earth-fault and phase relays benefit from the exact same process presented in section 4.2.2. Hence, in this section, only the process of obtaining the prompt settings for earth-fault relays is presented.

4.3.1 Prompt settings

Re-coordination of the earth-fault over-current relays benefits from the same strategy applied on the phase over-current relays. There are however, two differences on PTDS and RON. PTDS of earth-fault relays is obtained using equation (4.8).

$$PTDS = \frac{I^{0}_{TPOM}}{I^{0}_{DPOM}} \tag{4.8}$$

In equation (4.8), I^0_{TPOM} and I^0_{DPOM} represent zero-sequence current during TPOM and DPOM, respectively.

Despite phase over-current relays, earth-fault over-current relays coordination process is independent of the DPOM location. Hence, RON for the earth-fault over-current relays is a pre-determined variable and does not need the relay to calculate it based on the OBON. Considering that, earth-fault over-current relays also benefit from the t-I characteristic presented in equation (4.3) with the same value of TM as of the phase relays.

4.4 Performance evaluation

In this section, the re-coordination methodology for phase and earth-fault over-current relays presented in sections 4.2 and 4.3 is evaluated. The scenarios of DPOM presented in sections 3.3 and 3.5.1 are used to evaluate the proposed re-coordination methodology.

4.4.1 Phase over-current relays

This section focuses on re-coordination evaluation of the phase over-current relays. In section 3.3, three different scenarios of DPOM were presented and the necessity of re-coordination of these relays were clarified. The re-coordination results for these relays during the mentioned DPOM scenarios is presented below.

Radial network without DG units

In the first scenario, DPOM starts from bus B4 of the test system shown in figure 3.1. This means that breaker on phase A of feeder B3-B4 operates and sends a DPOM signal to the upstream relays along with the OBON. Following the re-coordination steps given in figure 4.1, upstream relays start calculation of RON using equation (4.2). At the same time, the relays measure the new current flowing through phase A. By measuring the new phase current and using the TPOM phase current stored in the relay, PTDS is obtained using equation (4.1). If the obtained PTDS is equal to 1, it means that the current flowing through the relay during DPOM and TPOM is the same. This means that the relay is not experiencing any change on the normal operation current and thus, the TPOM settings will be valid on that particular relay. The new pickup setting will also be calculated after obtaining the new phase current during DPOM and multiplying it by a factor of 1.2 in this project. Now that the new pickup setting and the PTDS is calculated, the relay updates the new settings and will be able to protect the system during DPOM. Table 4.1 tabulates the prompt settings obtained by the relays for this scenario.

As shown in table 4.1, in this DPOM scenario, three phase over-current relay are affected which are relays B0-B1, B1-B2 and B2-B3. For these relays, B2-B3 is the most downstream relay and RON of this relay is assigned to 1. The next relays, B1-B2 and B0-B1 are the next two relays in this system with RON 2 and 3, respectively.

Figure 4.2 depicts the t-I curves of the re-coordinated relays with prompt settings applied on the relays. As shown in figure 4.2, the relays are well-coordinated and able to protect the

Table 4.1: Prompt settings for phase A relays during first scenario of DPOM. Switch S3 in figure 3.1 is open and no DG is connected to the network.

Relay	$I_{\phi A_{3\phi}}$ (kA)	$I_{\phi A_{2\phi}}$ (kA)	PTDS	I_{Pickup} (kA)	RON
B0-B1	0.246	0.176	0.7	0.21	3
B1-B2	0.221	0.151	0.68	0.18	2
B2-B3	0.177	0.107	0.6	0.12	1

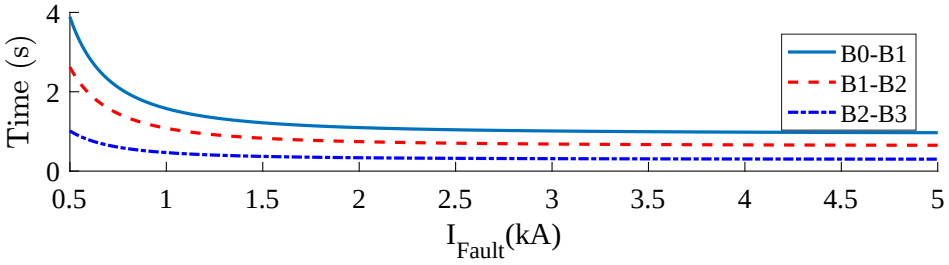

Figure 4.2: Re-coordinated phase relays for the first scenario of DPOM using prompt settings.

distribution feeder during DPOM.

After applying prompt settings on the relays and guaranteeing the protection of the system from beginning moments of DPOM, the relays start communicating the new characteristics of the system to the MCDC. These information include the phase current and the RON for phase relays. When the communication process between MCDC and the relays finishes, optimization process starts to find the optimum TDS setting for the relays that minimizes the operation

Table 4.2: Optimum settings for phase A relays during first scenario of DPOM. Switch S3 in figure 3.1 is open and no DG is connected to the network.

Relay	I_{Pickup} (kA)	TDS
B0-B1	0.21	3.6
B1-B2	0.18	3.2
B2-B3	0.12	2.7
B3-B8	0.115	1.9
B8-B9	0.08	1.6
B9-B10	0.06	1.1
B10-B11	0.035	0.5

time of the relays. Optimization process, as explained earlier in section 4.2.2, deploys NSGA II as optimization algorithm. Table 4.2 shows the results of the optimization process. The total operation time of the relays obtained by the optimization algorithm was recorded as 13.4 seconds.

Figure 4.3 shows the t-I curves of the optimized phase relays. As shown in this figure, the relays are coordinated and operate with the minimum operation time. These settings will be communicated to each relay from MCDC and will be updated on the relays.

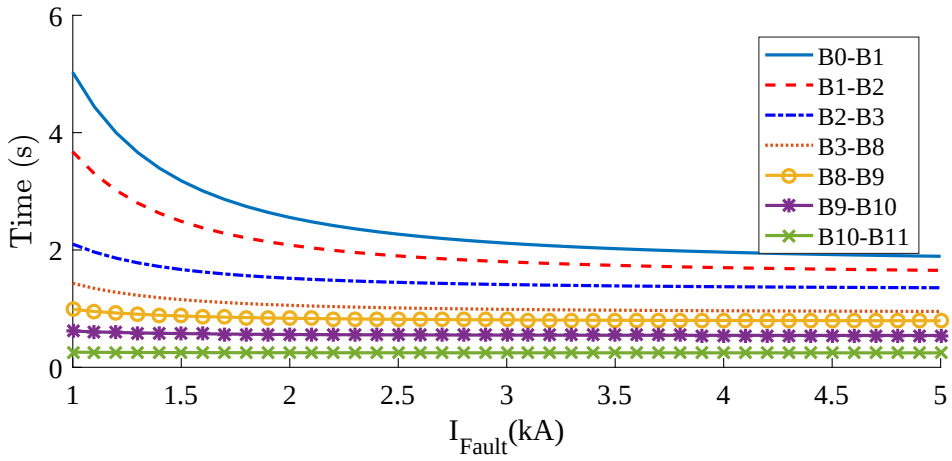

Figure 4.3: Optimized phase relays for the first scenario of DPOM.

Radial network with type 4 wind DG units

In this scenario, switch S3 in figure 3.1 remains open to keep the configuration of the network radial. The type 4 wind turbine is connected to bus B3, and DPOM starts from bus B8. This means that relays B8-B9, B9-B10 and B10-B11 are operating in DPOM and relays B3-B8, B2-B3, B1-B2 and B0-B1 operate in TPOM and affected by DPOM. Following the re-coordination process depicted in figure 3.4, the prompt settings will be obtained for relays operating in TPOM. Table 4.3 shows the prompt settings for this scenario.

As shown in this scenario, current flowing through phase A on upstream relays increases during DPOM due to the power injection of the DG unit to the main grid. However, the proposed re-coordination methodology is able to re-coordinate the phase over-current relays in this circumstances. Figure 4.4 shows the t-I curve of the re-coordinated relays.

Table 4.3: Prompt settings for phase A relays during second scenario of DPOM. Switch S3 is open and a type 4 wind turbine is connected to bus B3.

Relay	$I_{\phi A_{3\phi}}$ (kA)	$I_{\phi A_{2\phi}}$ (kA)	PTDS	I_{Pickup} (kA)	RON
B0-B1	0.085	0.091	1.1	0.11	4
B1-B2	0.085	0.1	1.2	0.12	3
B2-B3	0.093	0.125	1.4	0.15	2
B3-B8	0.096	0.03	0.3	0.036	1

After updating the relays of the system with prompt settings, optimization process for obtaining optimum settings for the relays starts by communicating the new network information measured by the relays to MCDC. Table 4.4 shows the optimum settings of the affected relays by DPOM for this scenario. The operation time obtained by the optimization algorithm is 4.94 s.

Figure 4.5 depicts the t-I curves of the optimized relays for this scenario. As shown, the relays are coordinated and guarantees the protection of the system.

Meshed network with type 4 wind DG units

In this scenario, switch S3 in figure 3.1 is closed to connect bus B4 to bus B11. This makes a loop starting from bus B3 to buses B8, B9, B10, B11, B4 and returns back to bus B3. The type 4 wind

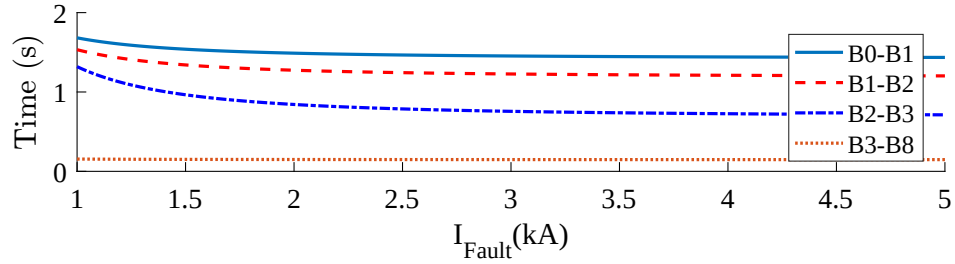

Figure 4.4: Re-coordinated phase relays for the second scenario of DPOM using prompt settings.

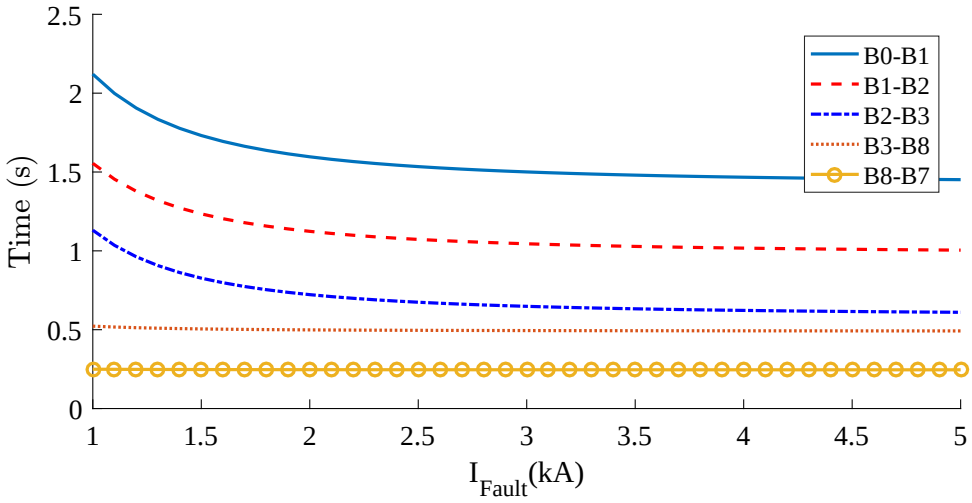

Figure 4.5: Re-coordinated phase relays for the second scenario of DPOM using prompt settings.

turbine is connected to bus B3, and DPOM starts from Bus B8. In this scenario, after operation of the breaker on feeder B3-B8, the relay B3 will be the most downstream relay on the feeder of B3-B8. From the other end, relay B9-B8 will be the fastest relay and re-coordination will be performed for these two coordination paths separately. Table 4.5 shows the prompt settings obtained by relays during DPOM.

In table 4.5, relays B0-B1, B1-B2 and B2-B3 PTDS is 1. This means that current flowing

Table 4.4: Optimum settings for phase A relays during second scenario of DPOM. Switch S3 in figure 3.1 is open and type 4 wind DG unit is connected to the network.

Relay	I_{Pickup} (kA)	TDS
B0-B1	0.11	2.9
B1-B2	0.12	2
B2-B3	0.15	1.2
B3-B8	0.04	1
B8-B7	0.02	0.5

through these relays does not change during DPOM. Hence, these three relays benefit from the TPOM settings and will not update with prompt settings. On the other hand, relays B3-B4, B4-B11, B11-B10, B10-B9 and B9-B8 experience significant change on the current flowing through these relays. Hence, re-coordination of these relays is necessary and prompt settings will be applied on the relays. Figure 4.6 shows the t-I curves of these relays updated by prompt settings.

Optimum setting will be obtained after deploying the prompt settings on the relays. Same as other scenarios, the relays will communicate with MCDC to transfer the necessary information for the optimization process. Table 4.6 shows the optimum settings for the relays affected by DPOM.

Table 4.5: Prompt settings for phase A relays during third scenario of DPOM. Switch S3 is closed and a type 4 wind turbine is connected to bus B3.

Relay	$I_{\phi A_{3\phi}}$ (kA)	$I_{\phi A_{2\phi}}$ (kA)	PTDS	I_{Pickup} (kA)	RON
B0-B1	0.1	0.1	1	0.12	N/A
B1-B2	0.096	0.096	1	0.12	N/A
B2-B3	0.096	0.096	1	0.12	N/A
B3-B4	0.1	0.14	1.4	0.17	5
B4-B11	0.027	0.066	2.5	0.08	4
B11-B10	0.02	0.036	1.8	0.05	3
B10-B9	0.024	0.015	0.63	0.018	2
B9-B8	0.04	0.03	0.25	0.036	1

In this scenario, there are two coordination paths for the relays. The first one starts from relays B0-B1, B1-B2, B2-B3, B3-B4, B4-B11, B11-B10 and B10-B9. The other path starts from relays B0-B1, B1-B2, B2-B3, B3-B4, B4-B5 and B5-B6. The total operation time of the relays obtained by the optimization process is 8.74 s and 11.8 s for the first and second coordination path, respectively. Figures 4.7 and 4.8 depict the t-I curves for the first and second coordination path, respectively.

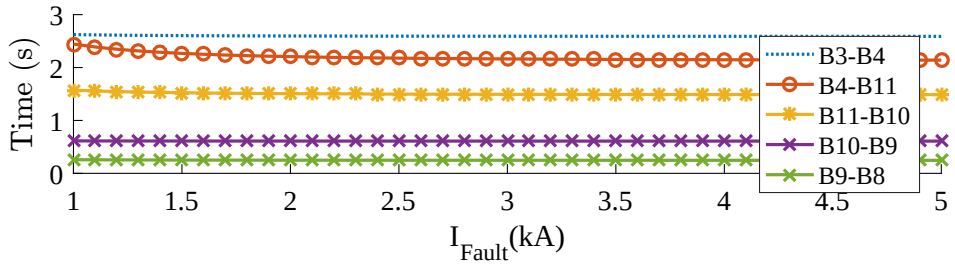

Figure 4.6: Re-coordinated phase relays for the third scenario of DPOM using prompt settings.

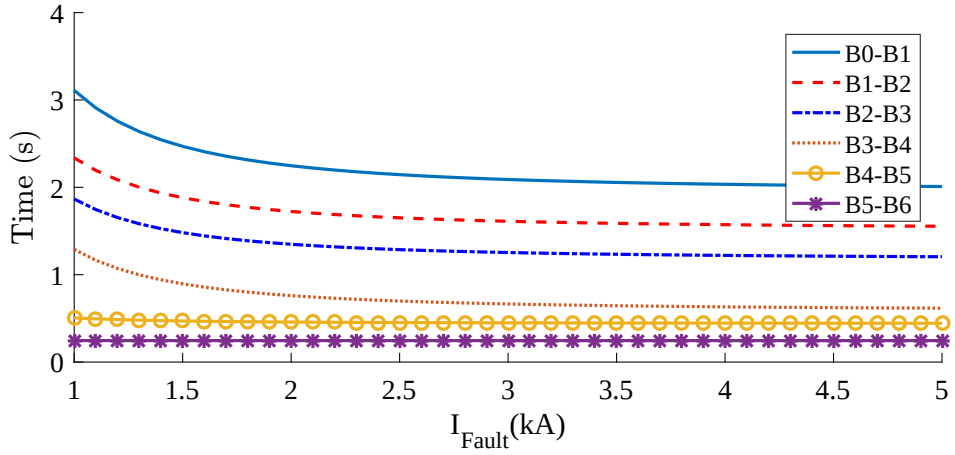

Figure 4.7: Optimized phase relays for the third scenario of DPOM for the first coordination path.

4.4.2 Earth-fault over-current relays

In this section, the re-coordination methodology for earth-fault over-current relays presented in section 4.3 is evaluated. To this aim, the three scenarios presented in section 3.5.1 are considered as the case studies for methodology evaluation purposes.

Table 4.6: Optimum settings for phase A relays during third scenario of DPOM. Switch S3 in figure 3.1 is closed and type 4 wind DG unit is connected to the network.

Relay	I_{Pickup} (kA)	TDS
B0-B1	0.12	4
B1-B2	0.115	3.1
B2-B3	0.2	2.4
B3-B4	0.17	1.6
B4-B5	0.06	0.9
B5-B6	0.008	0.5
B4-B11	0.08	1.4
B11-B10	0.045	0.9
B10-B9	0.02	0.5

Radial network without DG units

As the first scenario, DPOM starts from bus B4 as shown in figure 3.1. This means that breaker on phase A of feeder B3-B4 operates and sends a DPOM signal to all relays with the OBON. Following the re-coordination steps given in section 4.3, earth-fault relays start to obtain the

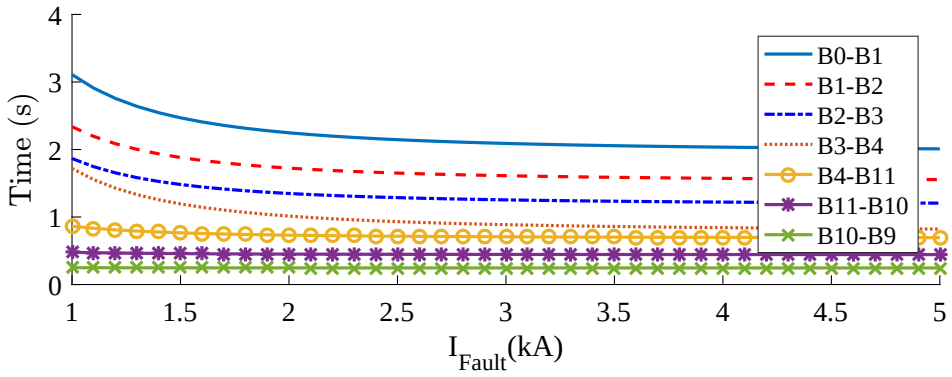

Figure 4.8: Optimized phase relays for the third scenario of DPOM for the second coordination path.

prompt settings. Table 4.7 shows the prompt settings obtained by relays for this DPOM scenario.

As shown in table 4.7, for relay B10-B11 PTDS is 1, meaning that DPOM does not affect the operation of this relay and thus, it benefits from the TPOM settings. Furthermore, there are two coordination paths in this system. The first one starts from relays B0-B1 to, B1-B2, B2-B3, B3-B4, B4-B5 and B5-B6. The second coordination path starts from relay B0-B1 and goes on to B1-B2, B2-B3, B3-B8, B8-B9 and B9-B10. Figure 4.9 shows the t-I curves of the re-coordinated earth-fault relays in the first coordination path with applied prompt settings on them.

Figure 4.10 shows the t-I curves of the re-coordinated earth-fault relays for the second coordination path in this scenario.

After applying the prompt settings on the earth-fault relays, communication between relays and MCDC starts to transfer the new measurements and starting the optimization process afterwards. The optimum settings are shown in table 4.8.

Table 4.7: Prompt settings for earth-fault relays during fist scenario of DPOM. Switch S3 in figure 3.1 is open and no DG unit is connected.

Relay	$I^o_{3\phi}$ (kA)	$I^o_{2\phi}$ (kA)	PTDS	New I^o_{Pickup} (kA)	RON
B0-B1	0.010	0.031	0.32	0.036	6
B1-B2	0.018	0.033	0.54	0.04	5
B2-B3	0.019	0.037	0.51	0.04	4
B3-B4	0.009	0.024	0.375	0.03	3
B4-B5	0.010	0.02	0.5	0.024	2
B5-B6	0.005	0.007	0.71	0.0084	1
B3-B8	0.007	0.006	1.16	0.007	4
B8-B9	0.002	0.003	0.66	0.004	3
B9-B10	0.004	0.009	0.44	0.011	2
B10-B11	0.002	0.002	1	0.003	1

Figure 4.11 depicts the t-I curves of the optimized earth-fault relays for the first scenario of DPOM and first coordination path. As shown in figure 4.11, the relays are coordinated and able to protect the system with the minimum operation time.

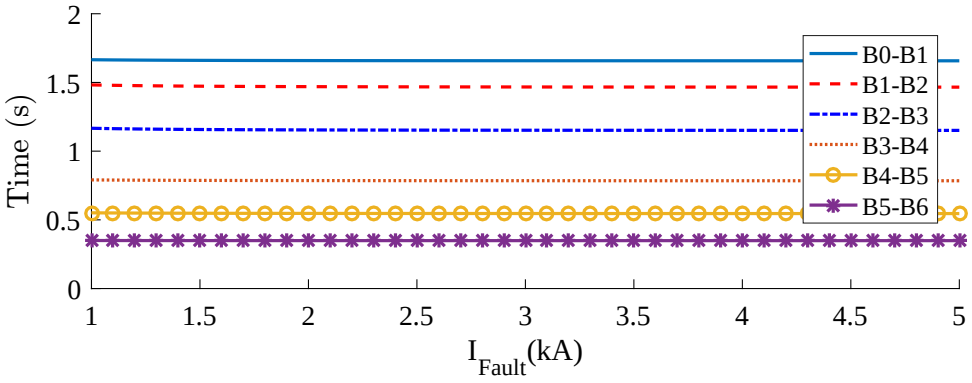

Figure 4.9: Prompt settings applied on earth-fault relays for the first scenario of DPOM for the first coordination path.

In figure 4.12, the t-I curves of the earth-fault relays for the second coordination path is depicted. Same as the first coordination path, the relays on second path also are coordinated and able to provide full protection for the system with the minimum operation time.

Radial network with type 4 wind DG unit

In this scenario, switch S3 in figure 3.1 remains open to keep the configuration of the network radial. The type 4 wind turbine is connected to bus B3, and DPOM starts from bus B8. DPOM signal will be sent to the relays and relays start to obtain the prompt settings based on the process presented in section 4.3. Table 4.9 shows the prompt settings for the earth-fault relays. In this scenario, there are two coordination paths. The first one starts from relays B0-B1 to, B1-B2, B2-B3, B3-B4, B4-B5 and B5-B6. The second coordination path starts from relay B0-B1 to B1-B2, B2-B3, B3-B8, B8-B9, B9-B10 and B10-B11. It worth to mention that RON for earth-fault over-current

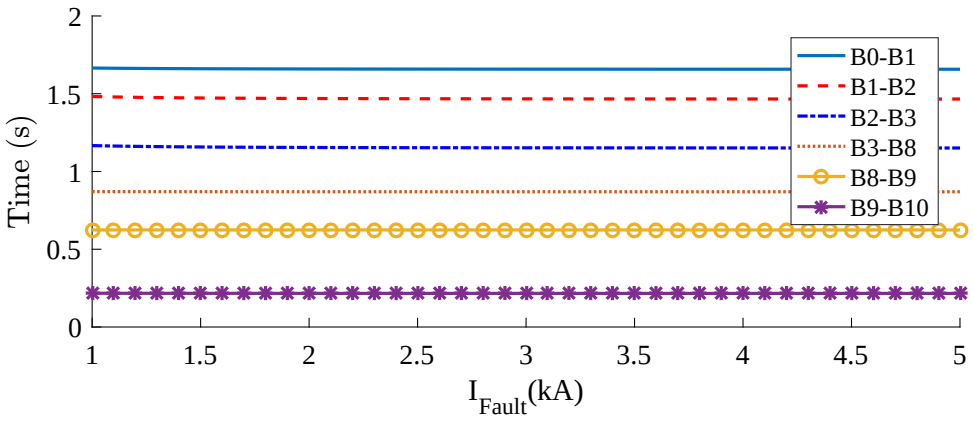

Figure 4.10: Prompt settings applied on earth-fault relays for the first scenario of DPOM for the second coordination path.

relays is independent from the OBON and is a constant number for each relay based on the location of the relays in the distribution feeder.

Figures 4.13 and 4.14 depict the t-I curve of the earth-fault relays updated with prompt settings for the first and second coordination path, respectively.

After obtaining the prompt settings, the relays start communicating the new measurements to the MCDC. Afterwards, MCDC begins the optimization process based on the process explained in section 4.2.2. Table 4.10 shows the optimum settings obtained by MCDC that minimizes the operation time of the earth-fault relays in this scenario.

After obtaining the optimum settings for the relays, MCDC transfers the new settings to each relay and relays will be updated with the new settings automatically. Figures 4.15 and 4.12 show the t-I curves of the earth-fault relays updated with the optimum settings.

Table 4.8: Optimum settings for earth-fault relays during fist scenario of DPOM. Switch S3 in figure 3.1 is open and no DG unit is connected.

Relay	I^{o}_{Pickup} (kA)	TDS
B0-B1	0.036	4.1
B1-B2	0.04	3.4
B2-B3	0.04	2.6
B3-B4	0.03	1.7
B4-B5	0.024	1.1
B5-B6	0.0084	0.5
B3-B8	0.007	2.3
B8-B9	0.004	1.7
B9-B10	0.011	1.1
B10-B11	0.003	0.5

As shown in figures 4.15 and 4.16, the relays are coordinated with settings that minimizes the total operation time of the relays of the system. The total operation time for the first and second coordination path were obtained as 10.5 s and 11.4 s, respectively.

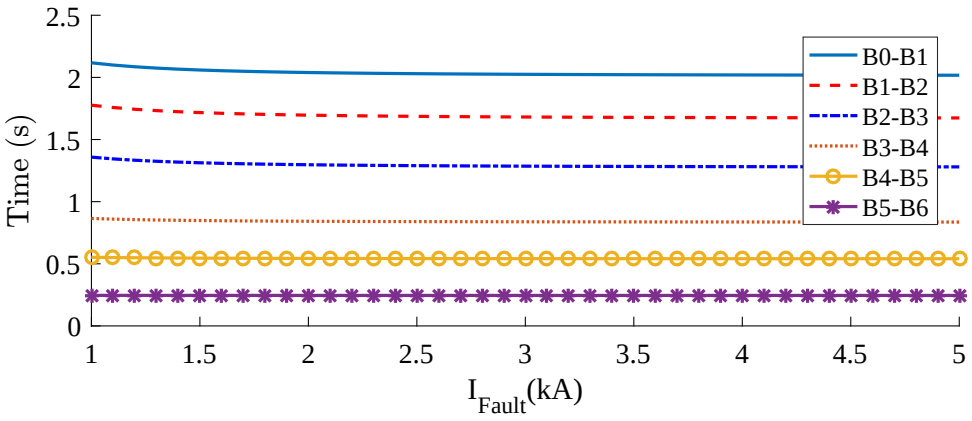

Figure 4.11: Optimum settings applied on earth-fault relays for the first scenario of DPOM for the first coordination path.

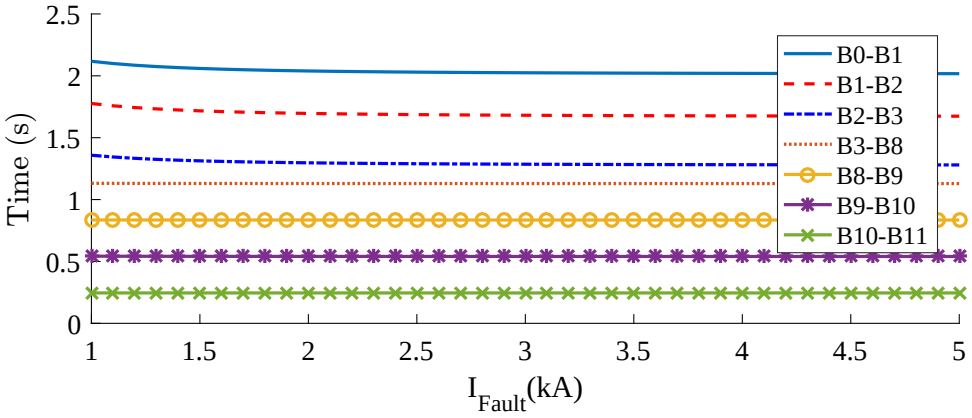

Figure 4.12: Optimum settings applied on earth-fault relays for the first scenario of DPOM for the second coordination path.

4.5 Conclusion

In this chapter, the proposed solution for re-coordination of the phase and earth-fault over-current relays was presented. The proposed solution has two critical factors that should be

Table 4.9: Prompt settings for earth-fault relays during second scenario of DPOM. Switch S3 in figure 3.1 is open and type 4 wind DG unit is connected.

Relay	$I^o_{3\phi}$ (kA)	$I^o_{2\phi}$ (kA)	PTDS	New I^o_{Pickup} (kA)	RON
B0-B1	0.03	0.01	3	0.012	6
B1-B2	0.008	0.011	0.72	0.013	5
B2-B3	0.009	0.014	0.64	0.017	4
B3-B4	0.011	0.01	1.1	0.012	3
B4-B5	0.005	0.01	0.5	0.012	2
B5-B6	0.007	0.007	1	0.008	1
B3-B8	0.001	0.03	0.03	0.04	4
B8-B9	0.004	0.023	0.17	0.03	3
B9-B10	0.002	0.017	0.11	0.02	2
B10-B11	0.005	0.008	0.625	0.01	1

considered:

- **Benefiting from local measurement**

  Local measurement is referred to the parameters that a relay measures. These parameters

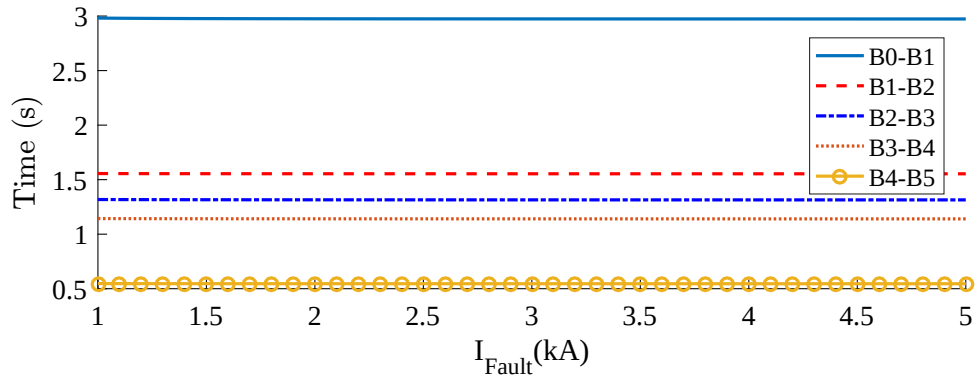

Figure 4.13: Prompt settings applied on earth-fault relays for the second scenario of DPOM for the first coordination path.

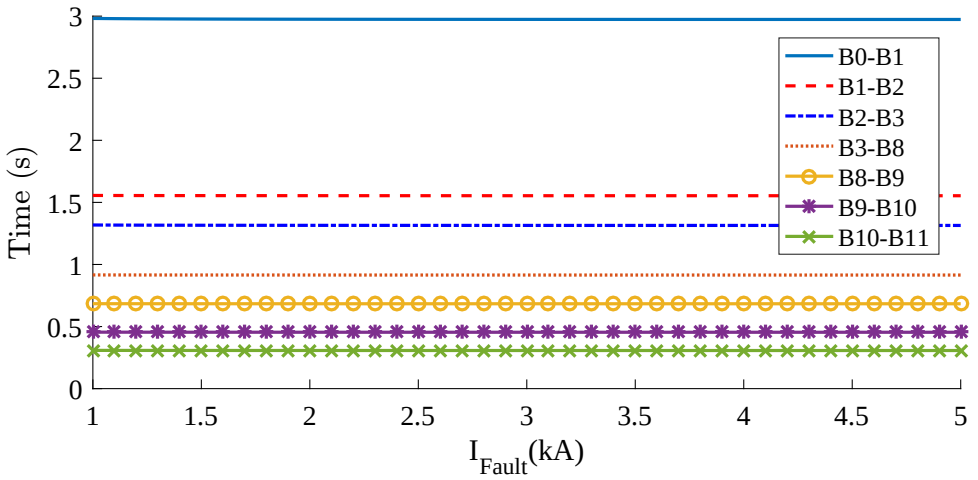

Figure 4.14: Prompt settings applied on earth-fault relays for the second scenario of DPOM for the second coordination path.

include load current, sequence currents, busbar voltage and so on. The main parameter that is used for coordination of phase or sequence over-current relays is the load current and sequence currents, respectively. By benefiting from locally measured network

Table 4.10: Optimum settings for earth-fault relays during second scenario of DPOM. Switch S3 in figure 3.1 is open and type 4 wind DG unit is connected to the network.

Relay	I^{o}_{Pickup} (kA)	TDS
B0-B1	0.011	4.1
B1-B2	0.014	3.3
B2-B3	0.017	2.7
B3-B4	0.012	1.8
B4-B5	0.012	1
B5-B6	0.006	0.5
B3-B8	0.004	2.2
B8-B9	0.03	1.6
B9-B10	0.02	1.1
B10-B11	0.01	0.5

parameters, the necessary information for setting the relays during DPOM is provided.

- **Fast and reliable**

  It is vital to have the relays coordinated as soon as DPOM starts. Otherwise, the system will

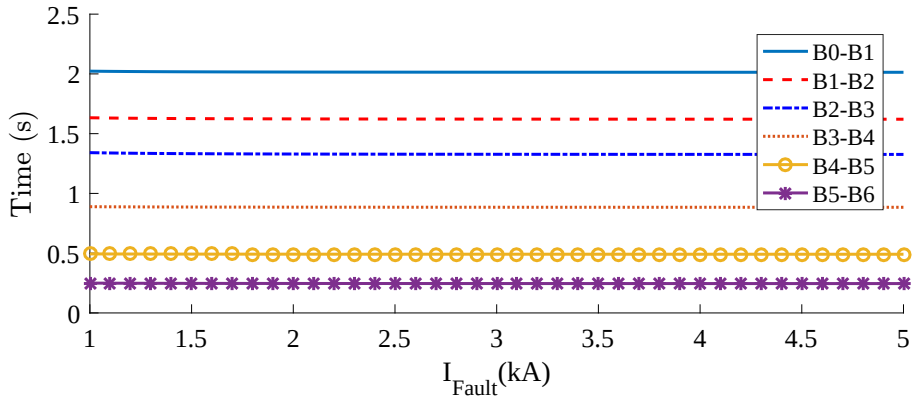

Figure 4.15: Optimum settings applied on earth-fault relays for the second scenario of DPOM for the first coordination path.

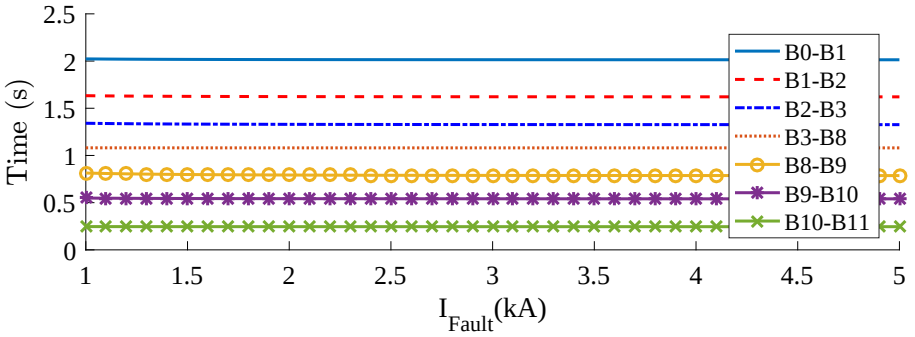

Figure 4.16: Optimum settings applied on earth-fault relays for the second scenario of DPOM for the second coordination path.

be left unprotected. Hence, the provided solution for re-coordination of the relays should be fast to guarantee the protection of the system.

The aforementioned factors have direct effect on the two sets of solution introduced in this project for re-coordination of the over-current relays, named as "Prompt settings" and "Optimum

settings".

Prompt settings guarantees the protection of the system from the first moment that DPOM starts. These settings are obtained by benefiting from local measurements as well as the DPOM start location. These settings are available on the relays temporarily until the optimum settings are obtained.

The process of calculating the optimum settings starts right after applying the prompt settings to the relays and communicating the new network parameters measured by relays like phase and zero-sequence current to the MCDC. MCDC begins the optimization process and after obtaining the optimum settings, the relays will be updated with the new settings. The optimum settings guarantee the minimum operation time of the relays.

The proposed solution was evaluated for different scenarios of DPOM. These scenarios covers all possible configurations of a distribution feeder such as, radial network, radial network with presence of DG unit, meshed network and meshed network with presence of DG unit. Based on the obtained settings for these scenarios, the re-coordination of the relays were successfully accomplished.

Chapter 5

Conclusions

5.1 Summary

The challenges caused by DPOM of distribution system on protective devices, exclusively phase over-current and earth-fault over-current relays were studied in this research. The studies were based on the simulation of the CIGRE North American medium-voltage distribution system benchmark [12] in PSCAD/EMTDC. The objectives of this research can be summarized as follow:

1. **Investigating the challenges caused by DPOM on over-current relays.**

2. **Proposing a new re-coordination methodology for the relays during DPOM.**

Contribution of this thesis leaded to accomplishing the objectives of this research which is

summarized in next section.

5.2 Contributions

To find the challenges caused by DPOM on operation of the over-current relays different scenarios of DPOM were studied on the project test system. The investigations showed that the following challenges the operation of the over-current relays:

- **Phase over-current relays**
  - **Change in current flowing through the relay**

    DPOM changes the configuration of the network and this leads to change in the current flowing through the relays. By this saying, the pickup settings during TPOM will not be applicable on the relays during DPOM should there is a change in the current flowing through the relay. This means that the pickup setting should be updated during DPOM.
  - **Change in the RON**

    Relay order number changes during DPOM for the upstream relays which protect the disconnected phase. RON is one of the main parameters that obtains the proper TDS setting for the relays.
- **Earth-fault over-current relays**

– **Change in zero-sequence current**

Zero-sequence current flowing through earth-fault relays changes as the result of DPOM. DPOM causes unbalanced load on the buses which leads to increment in the level of zero-sequence current. Malfunction of this type of relay is very likely during DPOM with TPOM settings.

By highlighting the challenges caused by DPOM on operation of the over-current relays, a solution should be provided for re-coordination of the relays during DPOM.

5.3 Proposal of solutions

After obtaining the changes caused by DPOM on operation of the over-current relays, a new methodology should be presented to re-coordinate the relays during DPOM. This methodology should be capable of obtaining new settings for the relays promptly based on the new network parameters. Two critical factors must be considered in this methodology:

- **Benefiting from local measurement**

  Local measurement is referred to the parameters that a relay measures. These parameters include load current, sequence currents, busbar voltage and so on. The main parameters that are used for coordination of phase or zero-sequence over-current relays are the load current and zero-sequence currents, respectively. By benefiting from locally measured

network parameters, the necessary information for setting the relays during DPOM is provided.

- **Fast and reliable**

  It is vital to have the relays coordinated as soon as DPOM starts. Otherwise, the system will be left unprotected. Hence, the provided solution for re-coordination of the relays should be fast to guarantee the protection of the system.

To achieve the new settings based on the aforementioned factors, two sets of settings is proposed to be applied on the relays during DPOM.

- **Prompt settings**

  To ensure that the protective relays are capable of protecting the system from the first moment that DPOM starts, a prompt setting should be obtained by the relay based on the local measurements and DPOM start location. Prompt settings are the temporary settings that are available on the relays until the optimum settings are obtained and updated on all the relays of the network.

- **Optimum settings**

  By applying the prompt settings on the relays of the network, the security of the system is ensured, however, the prompt settings are not necessarily the optimum settings that could be applied to the relays. Optimum settings in this project refer to the settings that minimize the operation time of the relays in the system.

These two sets of settings guarantee the correct operation of the over-current relays during DPOM and hence, the protection of the distribution system. The proposed solutions are practical to apply on the distribution systems for the following reasons:

1. **Applicable on all digital relays**

   The proposed solution is applicable to the digital relays available in the industry since it does not ask for a hardware change on the relays. The logic and the equations proposed as the new t-I curves for the relays can be uploaded on the digital relays.

2. **Low bandwidth communication**

   The communication between the relays and relays and MCDC can be obtained by using a low bandwidth communication scheme which is available on the modern digital relays.

5.4 Future work

Further research on operation analysis of protective relays during DPOM may include the following topics.

1. **Addressing the effects of DPOM on directional elements**

   DPOM can affect the operation of negative-sequence directional elements. Negative-sequence directional elements are used in networks with bidirectional flow of fault current. This element helps over-current relays to operate for the flow of current for which they are

applied. A comprehensive analysis should be performed on the operation of this element during DPOM.

2. **Addressing the effects of DPOM on transformer protection**

   DPOM can cause load unbalance on the disconnected phase of the distribution feeder and thus, unbalanced load connected to the transformers downstream of the DPOM start point. This can cause malfunction of the transformer protective relays like differential relays. This can be another topic for further research in investigating the effects of DPOM on distribution system protection system.

Bibliography

[1] J. R. Aguero, J. Wang, and J. J. Burke, "Improving the reliability of power distribution systems through single-phase tripping," in *IEEE PES T D 2010*, April 2010, pp. 1–7.

[2] T. S. Fahey and N. V. Burbure, "Single-phase tripping," *IEEE Power and Energy Magazine*, vol. 6, no. 2, pp. 46–52, March 2008.

[3] M. T. Bishop, C. A. McCarthy, and J. Josken, "Considering reliability in the selection of distribution system overcurrent protection devices," in *2000 Rural Electric Power Conference. Papers Presented at the 44th Annual Conference (Cat. No.00CH37071)*, 2000, pp. A3/1–A3/5.

[4] R. M. Cheney, J. T. Thorne, and G. Hataway, "Distribution single-phase tripping and reclosing: Overcoming obstacles with programmable recloser controls," in *2009 Power Systems Conference*, March 2009, pp. 1–10.

[5] ——, "Distribution single-phase tripping and reclosing: Overcoming obstacles with programmable recloser controls," in *2009 62nd Annual Conference for Protective Relay Engineers*, March 2009, pp. 214–223.

[6] J. John J. Grainger, William D. Stevenson, *Power System Analysis*. McGraw-Hill, 1994.

[7] A. Brameller and R. S. Pandey, "General fault analysis using phase frame of reference," *Electrical Engineers, Proceedings of the Institution of*, vol. 121, no. 5, pp. 366–368, May 1974.

[8] L. Roy and N. D. Rao, "Exact calculation of simultaneous faults involving open conductors and line-to-ground short circuits on inherently unbalanced power systems," *IEEE Power Engineering Review*, vol. PER-2, no. 8, pp. 47–48, Aug 1982.

[9] L. Roy and N. d. Rao, "Exact calculation of simultaneous faults involving open conductors and line-to-ground short circuits on inherently unbalanced power systems," *IEEE Transactions on Power Apparatus and Systems*, vol. PAS-101, no. 8, pp. 2738–2746, Aug 1982.

[10] I. N. D.P Kothari, *Modern Power System Analysis*. Tata McGraw-Hill, 1994.

[11] J. John J. Grainger, William D. Stevenson, *Power System Analysis*. McGraw-Hill, 1994.

[12] K. Strunz, "Benchmark systems for network integration of renewable and distributed energy resources," in *CIGRE Task Force C6.04.02*, August 2008.

[13] T. W. Ross and H. G. Bell, "Recent developments in the protection of three-phase transmission lines and feeders," *Electrical Engineers, Journal of the Institution of*, vol. 68, no. 403, pp. 801–823, July 1930.

[14] J. L. Blackburn and W. E. Glassburn, "A new line of protective relays and cases," *Electrical Engineering*, vol. 76, no. 3, pp. 215–215, March 1957.

[15] F. P. Brightman, "Selecting a-c overcurrent protective device settings for industrial plants," *Transactions of the American Institute of Electrical Engineers, Part II: Applications and Industry*, vol. 71, no. 4, pp. 203–211, Sept 1952.

[16] T. J. D. J. Lewis Blackburn, *Protective Relaying Principles and Applications*. CRC Press, 2006.

[17] *IEEE Standard inverse-Time Characteristics Equations for Overcurrent Relays*, IEEE Std., 1997.

[18] *Manual: SEL-751 Relay, Feeder Protection Relay*, SCHWEITZER ENGINEERING LABORATORIES, INC., Washington, Dec. 2017. [Online]. Available: https://selinc.com/products/751/

[19] *Manual: SEL-351-5,-6,-7 Protection System*, SCHWEITZER ENGINEERING LABORATORIES, INC., Washington, Dec. 2017. [Online]. Available: https://selinc.com/products/351/

[20] *Manual: ABB Distribution Protection Unit 2000R*, ABB, March. 2004. [Online]. Available: http://new.abb.com/medium-voltage/distribution-automation/numerical-relays/feeder-protection-and-control/other-series/distribution-protection-unit-2000r-dpu2000r

[21] *Manual: ABB Micro51 Microporcessor-Based Overcurrent Relay*, ABB, April. 2004. [Online]. Available: http://new.abb.com/medium-voltage/distribution-automation/numerical-relays/feeder-protection-and-control/other-series/microprocessor-based-time-overcurrent-relay---micro-51

[22] K. Zimmerman, "Microprocessor-based distribution relay applications," in *American Public Power Association's Engineering and Operations Workshop*. Schweitzer Engineering Laboratories, Inc.

[23] J. A. S. Mark D.Diehl, Robert A. Crognale, "Microprocessor relay capabilities improve protection, scada and maintenance," in *25th Annual Western Protective Relay Conference*. Schweitzer Engineering Laboratories, Inc.

[24] "Network protection and automation guide, protective relays, measurement and control," May. 2011.

[25] J. S. T. Arun G. Phadke, *Computer Relaying for Power System*. WILEY, 2009.

[26] S. A. H. S. Olia, M. Jooshaki, M. Moeini-Aghtaie, and M. Fotuhi-Firuzabad, "Developing a multi-objective framework for planning studies of modern distribution networks," in *2016 International Conference on Probabilistic Methods Applied to Power Systems (PMAPS)*, Oct 2016, pp. 1–6.

[27] K. Saleh, H. Zeineldin, A. Al-Hinai, and E. El-Saadany, "Optimal coordination of directional overcurrent relays using a new time-current-voltage characteristic," in *2016 IEEE Power and Energy Society General Meeting (PESGM)*, July 2016, pp. 1–1.